Measurement of the inclusive isolated prompt photon cross section in pp collisions at $\sqrt{s} = 8$ TeV with the ATLAS detector

The ATLAS collaboration

E-mail: atlas.publications@cern.ch

ABSTRACT: A measurement of the cross section for the inclusive production of isolated prompt photons in proton-proton collisions at a centre-of-mass energy of $\sqrt{s} = 8$ TeV is presented. The measurement covers the pseudorapidity ranges $|\eta^\gamma| < 1.37$ and $1.56 \leq |\eta^\gamma| < 2.37$ in the transverse energy range $25 < E_T^\gamma < 1500$ GeV. The results are based on an integrated luminosity of $20.2\,\text{fb}^{-1}$, recorded by the ATLAS detector at the LHC. Photon candidates are identified by combining information from the calorimeters and the inner tracker. The background is subtracted using a data-driven technique, based on the observed calorimeter shower-shape variables and the deposition of hadronic energy in a narrow cone around the photon candidate. The measured cross sections are compared with leading-order and next-to-leading order perturbative QCD calculations and are found to be in a good agreement over ten orders of magnitude.

Contents

1 Introduction

Prompt photons, excluding those originating from hadron decays, are produced at the LHC in the hard process $pp \rightarrow \gamma + X$. The measurement of this inclusive production provides a probe of perturbative Quantum Chromodynamics (pQCD) and specifically, through the dominant leading-order (LO) process $qg \rightarrow q\gamma$, can be used to study the gluon parton distribution function (PDF) [1–6] of the proton. In addition, an improved understanding of prompt photon production is potentially important in aiding analyses of processes for which they are an important background (for instance, measurements of the Higgs boson in the diphoton decay channel).

Inclusive prompt photon production is made up of two contributions: direct and fragmentation photons. Direct photons are those associated with the hard sub-process, whereas fragmentation photons are produced from the fragmentation of a coloured parton. An isolation requirement is used to reduce both the poorly understood non-perturbative fragmentation contribution and the contamination from the dominant background of photons originating from hadron decays, mainly light neutral mesons (i.e. π^0, η).

Inclusive measurements of prompt photons have been made at hadron colliders by ATLAS [7–9], CMS [10, 11], CDF [12], D0 [13, 14], UA1 [15] and UA2 [16]. The analysis presented here uses 20.2 fb^{-1} of proton-proton collision data recorded by the ATLAS detector and is performed at a higher centre-of-mass energy (8 TeV) than the previous measurements. Similar measurements have also been made previously in deep inelastic scattering and photoproduction experiments at HERA [17–20].

The fiducial region of the measurement presented is defined in terms of the photon kinematic quantities:[1] transverse energy E_T^γ, pseudorapidity η^γ and transverse isolation energy E_T^{iso}. The differential cross section is measured as a function of E_T^γ, for the highest-energy photon in the event, and spans the $25 < E_T^\gamma < 1500$ GeV range. The η^γ range is split to give four intervals for the cross-section measurement: $|\eta^\gamma| < 0.6$, $0.6 \le |\eta^\gamma| < 1.37$, $1.56 \le |\eta^\gamma| < 1.81$ and $1.81 \le |\eta^\gamma| < 2.37$. The final constraint is the photon isolation, where E_T^{iso} is calculated within a cone of size $\Delta R = 0.4$, centred around the photon, and is chosen to be $E_T^{iso} < 4.8$ GeV $+ 4.2 \times 10^{-3} \times E_T^\gamma$. This fiducial region is identical in both the theoretical calculations and the experimental measurement; however, there are differences in the calculation of E_T^{iso}:

- At detector level it is the sum of energy deposits in the calorimeter, corrected for the deposits related to the photon candidate itself.

- At particle level it is the sum of energy from all particles, except for muons, neutrinos and the photon itself.

- At parton level it is the sum of energy from all coloured partons.

An additional correction to remove energy from the underlying event (UE) or additional proton-proton interactions is applied at detector and particle level, as detailed in section 4.2.

There are several differences between the measurement presented here and the previous ATLAS inclusive photon measurements [7–9]. In addition to the change in centre-of-mass energy and E_T^γ reach, it also probes for the first time the region $25 < E_T^\gamma < 45$ GeV for $1.81 \le |\eta^\gamma| < 2.37$. The measurement is also compared to different theoretical predictions than used previously, as detailed in section 3. An E_T^γ-dependent isolation requirement is introduced for the first time, effectively relaxing the maximum E_T^{iso} at high E_T^γ, as outlined in section 4 along with the discussion of changing the upper edge of the excluded η^γ region from 1.52 to 1.56. Other differences in the background estimation, unfolding and uncertainty calculations are highlighted in sections 5, 6 and 7 respectively, and the results are shown in section 8.

2 ATLAS detector and data

The ATLAS experiment [21] at the LHC is a multi-purpose particle detector with a forward-backward symmetric cylindrical geometry and a near 4π coverage in solid angle. It consists

---

[1] ATLAS uses a right-handed coordinate system with its origin at the nominal interaction point (IP) in the centre of the detector and the z-axis along the beam pipe. The x-axis points from the IP to the centre of the LHC ring, and the y-axis points upwards. Cylindrical coordinates (r, ϕ) are used in the transverse plane, ϕ being the azimuthal angle around the z-axis. The pseudorapidity is defined in terms of the polar angle θ as $\eta = -\ln\tan(\theta/2)$. Angular distance is measured in units of $\Delta R \equiv \sqrt{(\Delta\eta)^2 + (\Delta\phi)^2}$.

of an inner tracking detector surrounded by a thin superconducting solenoid providing a 2 T axial magnetic field, electromagnetic and hadronic calorimeters, and a muon spectrometer. The inner tracking detector covers the pseudorapidity range $|\eta| < 2.5$. It consists of silicon pixel, silicon microstrip, and transition radiation tracking detectors. Within the region $|\eta| < 3.2$, EM calorimetry is provided by high-granularity lead/liquid-argon (LAr) sampling calorimeters, with an additional thin LAr presampler covering $|\eta| < 1.8$, to correct for energy loss in material upstream of the calorimeters. A hadronic (steel/scintillator-tile) calorimeter covers the central pseudorapidity range ($|\eta| < 1.7$). The end-cap and forward regions are instrumented with LAr calorimeters for both the EM and hadronic energy measurements up to $|\eta| = 4.9$. The muon spectrometer surrounds the calorimeters and is based on three large air-core toroid superconducting magnets with eight coils each. It includes a system of precision tracking chambers and fast detectors for triggering. A three-level trigger system is used to select events. The first-level trigger is implemented in hardware and uses a subset of the detector information to reduce the accepted rate to at most 75 kHz. This is followed by two software-based high-level triggers that together reduce the accepted event rate to 400 Hz on average, depending on the data-taking conditions during 2012.

The dataset used in this analysis was obtained using proton-proton collisions recorded in 2012 by the ATLAS detector, when the LHC operated at a centre-of-mass energy of $\sqrt{s} = 8$ TeV. The integrated luminosity of the dataset used in this measurement is 20.2 fb^{-1}with an uncertainty of 1.9% [22]. The events used in the analysis were recorded by the trigger system using single-photon triggers [23], which use identification criteria looser than the selection described in section 4.1. For the high-level triggers, $E_{\rm T}^{\gamma}$ thresholds are defined in 20 GeV steps from 20 GeV to 120 GeV. Multiple trigger thresholds are required because the triggers are prescaled to reduce their rate, except for the unprescaled 120 GeV threshold. Each threshold is used in the analysis within an exclusive $E_{\rm T}^{\gamma}$ range, determined to be where the trigger has an efficiency greater than 99.5%, with respect to the full selection detailed in section 4. Only events taken during periods of good data quality, where the calorimeters and inner tracking detectors are in nominal operation, are retained in the dataset. To remove any non-collision background, each event is required to have a reconstructed vertex consistent with the average beam-spot position, where the vertex is required to have at least two associated tracks. This condition is close to 100% efficient for retaining events with photons within the detector acceptance.

3 Theoretical predictions

The theoretical calculations used in the analysis consist of LO Monte Carlo (MC) event generators and calculations at next-to-leading-order (NLO) or higher. Two event generators are used at LO: PYTHIA 8.165 [24] and SHERPA 1.4.0 [25]. These event generators are interfaced with a detailed detector simulation [26] (based on GEANT4 [27]), the output of which is reconstructed in the same way as the data. The LO predictions are used to study many aspects of the analysis and are also compared to the final cross section. The final

cross sections are also compared to three calculations: JETPHOX [28], PETER [29, 30][2] and MCFM [31].[3]

Event generation with PYTHIA includes: the description of the PDFs using CTEQ6L1 [32], the simulation of initial- and final-state radiation, the simulation of the UE using the ATLAS AU2 set of tuned parameters (tune) [33] based on the multiple parton interaction model [34], and the modelling of the hadronisation based on the Lund string model [35]. The LO direct contribution to the prompt photon production is fully included in the main matrix-element calculation. In contrast, the fragmentation contribution is modelled by final-state QED radiation arising from calculations of all $2 \rightarrow 2$ QCD processes.

PYTHIA is used to extract the central values of the measurement, while SHERPA is used as a second LO generator as it showed excellent agreement with the results in the ATLAS photon plus jet measurement [36]. The SHERPA predictions are used to cross-check the results and determine uncertainties arising from the use of MC simulations in parts of the analysis. The SHERPA calculations are performed with up to four parton emissions and the radiation of gluons and photons is done coherently. This means that the fragmentation contribution is produced differently to the contribution in PYTHIA and is also indistinguishable from the direct contribution, unlike PYTHIA where the contributions can be separated. The SHERPA events are produced with: the CT10 [37] PDF, the UE model based on the recommended tune provided by the SHERPA authors, and hadronisation modelled using a modified version of the cluster model [38].

The LO simulated events used in the analysis are reweighted in order to match as well as possible the experimental conditions of the dataset. One of these corrections is to reproduce the pile-up (additional proton-proton interactions in the same bunch crossing) conditions, where the weights are derived from the distribution of average interactions per bunch crossing (μ) in data and MC simulations with an additional constant to improve the agreement of the number of primary vertices. A second weight is used to ensure an accurate η^γ measurement by reproducing in the MC simulations the z-vertex position of the hard interaction measured in data.

The final cross sections are compared to these LO generators and also to parton-level calculations. The kinematic selection used in all of the predictions matches the fiducial region defined in section 1. For the higher order predictions the nominal renormalisation (μ_R), factorisation (μ_F) and fragmentation (μ_f) scales were set to the photon transverse energy ($\mu_R = \mu_F = \mu_f = E_T^\gamma$).

JETPHOX, a well-established NLO parton-level generator for the prediction of processes with photons in the final state, is used as the baseline to compare the results. JETPHOX is capable of calculating the double-differential inclusive prompt photon cross section $\mathrm{d}^2\sigma/(\mathrm{d}E_T^\gamma \mathrm{d}\eta^\gamma)$ at parton level to NLO accuracy for both the direct and fragmentation photon processes. The calculation can be configured to use an E_T^γ-dependent isolation

---

[2] We thank Matthew Schwartz for providing theoretical predictions for the inclusive photon cross section using the PETER calculation; http://peter.hepforge.org.

[3] We thank Ciaran Williams and John Campbell for their help in the ongoing investigation of the unexpected differences seen in the MCFM.

requirement[4] and uses the NLO photon fragmentation function of BFG set II [39, 40]. To check the effect of the PDF choice on the predictions, they are generated with different PDF sets (CT10, MSTW2008NLO [41], NNPDF2.3 [42] and HERAPDF1.5 [43]), provided by the LHAPDF package [44]. The strong coupling constant (α_S) is also obtained for each PDF using LHAPDF and the fine-structure constant (α_{EM}) is set to the JETPHOX default of 1/137.

The following systematic uncertainties (combined in quadrature) are assigned to the JETPHOX calculations and are estimated by means of procedures [45] used in the previous measurements:

- The uncertainty on the scale choice is evaluated from the envelope of varying the three scales by a factor of two around the nominal value, both simultaneously and independently (keeping two fixed at the nominal value). The impact on the predicted cross section varies between 12% and 20%.

- The PDF uncertainty is obtained by repeating the JETPHOX calculation for the 52 eigenvector sets of the CT10 PDF and applying a scaling factor in order to produce the uncertainty for the 68% confidence-level (CL) interval. The corresponding uncertainty in the cross section increases with E_T^γ and varies between 5% at 100 GeV and 15% at 900 GeV.

- The uncertainty due to α_S is evaluated, following the recommendation of ref. [37], by repeating the calculation with α_S varied by ± 0.002 around the central value of 0.118 and scaling in order to obtain the uncertainty for the 68% CL interval. The uncertainty due to α_S is smaller than that from the scale or PDF uncertainties for the whole phase space; it slowly decreases from 9% with increasing E_T^γ, with the exception of above 900 GeV where it increases to 15%.

- To be able to correct from parton level to particle level, additional hadronisation-plus-UE correction factors were evaluated using the two alternative hadronisation and UE models in PYTHIA and SHERPA. The study was performed by repeating the calculation with and without the hadronisation and UE contributions and resulted in a correction close to unity for both MC models with a small deviation of at most 2% at low E_T^γ. Therefore, as in the previous analyses, no correction factor is applied to the central value; however, in this measurement an E_T^γ-dependent uncertainty is assigned to the theory, based on the largest deviation from unity between the two models.

PETER is used as a second parton-level generator to predict the differential isolated prompt photon cross section at NLO including the resummation of threshold logarithms at the next-to-next-to-next-to-leading-logarithmic (NNNLL) level. PETER is roughly equivalent to a fixed-order calculation at next-next-to-leading-order (NNLO); there is currently no exact calculation available for inclusive photons at this order. To account for the isolation criteria applied in the measurement, the PETER result at NLO is normalised to that

---

[4]The E_T^{iso} requirement selected in this analysis is chosen to not be too restrictive for the NLO calculations, to avoid potential unphysical values in these predictions [28].

from JETPHOX. The PETER predictions are supplemented with the resummation of large electroweak Sudakov logarithms according to ref. [46, 47]. These electroweak corrections, not included in the predictions from JETPHOX, provide estimates of electroweak uncertainties that are important for high E_T^γ and also mean that, unlike JETPHOX, PETER uses a running α_{EM}. The scale uncertainty is calculated similarly to JETPHOX, by varying the scales around the central value, but in PETER there are four scales [48]: hard matching, jet, soft and factorisation. Finally the PDF uncertainty is taken directly from JETPHOX.

An additional study was made using MCFM, following on from the studies in ref. [49], with parameters (CT10 PDF, photon isolation, scale choice and α_{EM}) matching those in JETPHOX. MCFM calculates the fragmentation process only to LO and therefore deviations from JETPHOX predictions were expected below approximately 200 GeV. Surprisingly, however, even at higher E_T^γ the predictions from MCFM were found to be consistently below the predictions from JETPHOX, although within the theoretical uncertainties. This trend is under investigation by the calculations authors and the predictions are not presented here.

4 Photon selection

The photon selection, in both data and MC simulation, is based on the reconstruction [50] of an EM cluster in the calorimeter as a photon candidate. The absence of an associated track in the inner detector classifies the photon candidate as an *unconverted* photon, whereas it is classified as a *converted* photon if the cluster is matched to two tracks coming from a conversion vertex or to one track which has no hits in the innermost layer of the inner tracking detector. Both the converted and unconverted candidates are kept in the analysis. A further track-based classification [51] is used to minimise the number of electrons reconstructed as photons, although this introduces a slight decrease in efficiency for reconstructing converted photons. The conversion classification is used both to determine the size of the photon cluster in the barrel calorimeter and also as an input to the dedicated energy calibration [52], which is applied to account for energy loss before the EM calorimeter. This calibration starts by correcting the response from each of the layers in the EM calorimeter and then applies a response calibration from MC simulations to the cluster energies. After accounting for detector response variations not included in the simulation, such as high-voltage inhomogeneities in some sectors, energy scale factors are then applied from the comparison of the detector response to Z boson decays to electron-positron pair events in data and MC simulations.

Following this calibration, only photon candidates with $E_T^\gamma > 25$ GeV and a cluster barycentre (in the second layer of the EM calorimeter) lying within $|\eta^\gamma| < 1.37$ or $1.56 \leq |\eta^\gamma| < 2.37$ are retained for the analysis. The transition region between the barrel and end-cap calorimeters ($1.37 \leq |\eta^\gamma| < 1.56$) is excluded due to the degraded performance induced by the increased amount of inactive material in front of the calorimeter. This region is expanded in the measurement presented here to 1.56, compared to the value of 1.52 used previously, to improve the accuracy of the photon energy measurement as it avoids using clusters calibrated by scintillators that are part of the hadronic calorimeter.

Finally, photons reconstructed near regions of the calorimeter affected by read-out or high-voltage failures are not included in the analysis. The remaining photon candidates are then used in this analysis if they satisfy further selection and quality criteria based on their calorimeter shower shapes and isolation energy.

4.1 Photon identification

In order to reduce the previously mentioned largest background, namely non-prompt photons originating mainly from decays of energetic π^0 and η mesons, nine shower-shape variables [50] are exploited, similarly to the previous ATLAS inclusive photon measurements. These shower-shape variables are formed based on the relative and absolute energy deposition within the calorimeter cells using the full granularity of the different layers of the calorimeter system. The particular selection criteria for each of the nine variables are tuned for converted and unconverted photons separately, as well as being adjusted depending on η^γ (in intervals matching the four η^γ regions of this measurement). In the MC simulations the same criteria are applied as in data, but with two corrections. Firstly, the shower-shape variables are shifted [50] to match the measured distributions in data. Secondly, additional correction factors (at most a few percent from unity) to match the identification efficiency in the MC simulations and that in data are applied, calculated in each E_T^γ and η^γ interval.

To quantify the effect of the identification criteria, the identification efficiency for prompt photons is defined in MC simulations as:

$$\epsilon_{\mathrm{id}}^{\mathrm{MC}} = \frac{N_{\mathrm{id,matched}}^{\mathrm{MC}}}{N_{\mathrm{particle}}^{\mathrm{MC}}}. \tag{4.1}$$

where reconstructed photons have to satisfy the identification criteria and be geometrically matched, with $\Delta R < 0.2$, to isolated photons generated at particle level. This $\epsilon_{\mathrm{id}}^{\mathrm{MC}}$ is shown in figure 1 along with the efficiencies for converted and unconverted photons.[5] The unconverted photon efficiency is high and approximately constant for more energetic photons, as expected since they should leave a more pronounced shower in the detector. However, a drop in efficiency is observed when combining with converted photons. The efficiency to reconstruct conversions decreases at high E_T^γ (> 150 GeV) where it becomes more difficult to separate the two tracks from the conversions. These very close-by tracks are more likely to fail the tighter selections, including a transition radiation requirement, applied to single-track conversion candidates.

4.2 Photon isolation

The photon candidates are required to be isolated to distinguish between prompt photons and hadronic background. As stated in section 1, E_T^{iso} is calculated from topological clusters of calorimeter cells in a cone of size $\Delta R = 0.4$ around the photon and corrected for the deposits related to the photon candidate itself. As this quantity is susceptible to

---

[5]At particle level the conversion classification is based on information from the detailed detector simulation of the photon, by searching for a conversion of the photon into an electron-positron pair within the geometrical region of the inner tracking detector.
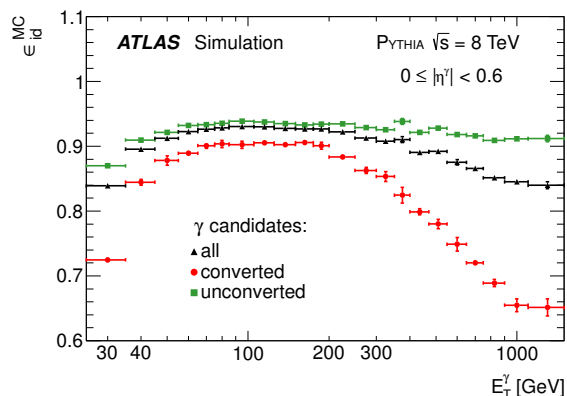
Figure 1. The photon identification efficiency (with statistical uncertainty) as a function of E_T^γ determined in PYTHIA MC simulations, along with the separated efficiencies for unconverted and converted photons. The efficiency is shown for the region $|\eta^\gamma| < 0.6$, with similar results found in other $|\eta^\gamma|$ regions.

contributions from the UE and pile-up, a correction based on the jet area method [53] is applied. This estimates on an event-by-event basis the ambient energy density, which is then subtracted from the E_T^{iso} before applying the isolation requirement. These corrections are typically between 1.5 and 2 GeV. In order for the detector-level E_T^{iso} distribution to reproduce the distribution from data, it is corrected in each E_T^γ and η^γ interval by the difference between the mean value of E_T^{iso} in data and MC simulations. These corrections range from a few hundred MeV up to 3-4 GeV and are consistent for both PYTHIA and SHERPA.

The measurement presented here uses an E_T^γ-dependent isolation requirement:

$$E_T^{iso} \; < \; 4.8 \;\; \text{GeV} \; + \; 4.2 \; \times \; 10^{-3} \; \times \; E_T^\gamma. \tag{4.2}$$

In contrast to the fixed value (3 or 7 GeV) used in the previous analyses, this requirement has been optimised to retain more of the photons satisfying the identification criteria in section 4.1 whilst also obtaining the best signal-to-background ratio throughout the large E_T^γ range of the measurement. In addition, the fraction of photon candidates that have satisfied the identification criteria and subsequently also satisfy the isolation requirement, stays high and constant. This is due to the isolation requirement being relaxed at higher E_T^γ, compared to using a fixed cut.

5 Background subtraction

The number of events with a photon candidate ($N^{\gamma,\text{data}}$) satisfying the kinematic, identification and isolation selection criteria, as detailed in section 4, has contributions from hadronic background and electrons. These contributions are removed statistically by techniques detailed below.

The hadronic background (from meson decays and jets) is removed by a data-driven technique, as done in the previous ATLAS analyses. This technique uses a two-dimensional

sidebands method based on the isolation and identification criteria. For the identification, photons either satisfy the full criteria of all the shower-shape variables outlined in section 4.1 or an orthogonal selection which aims to maximise the hadronic background. This orthogonal selection is achieved by inverting four variables related to the first layer of the EM calorimeter, which has cells with a very small width in η. For isolation, photons are either isolated as defined in section 4.2 or non-isolated by having $E_{\mathrm{T}}^{\mathrm{iso}} > 7.8$ GeV $+ 4.2 \times 10^{-3} \times E_{\mathrm{T}}^{\gamma}$. The four regions are then defined in data to be:

- $N^{A,\mathrm{data}}$: photon candidates satisfying both the isolation and identification criteria, i.e. $N^{\gamma,\mathrm{data}}$.

- $N^{B,\mathrm{data}}$: photon candidates that are non-isolated, but satisfy the identification criteria.

- $N^{C,\mathrm{data}}$: photon candidates that only satisfy the orthogonal identification criteria but are isolated.

- $N^{D,\mathrm{data}}$: photon candidates that only satisfy the orthogonal identification criteria and are non-isolated.

As defined above, there is a 3 GeV separation between the non-isolated region and the isolated region. This separation is used to limit the number of particle-level signal photons that fall into the background regions. To quantify this effect, signal leakage fractions are calculated in MC simulations:

$$f^{K,\mathrm{MC}} = \frac{N_{\mathrm{signal}}^{K,\mathrm{MC}}}{N_{\mathrm{signal}}^{A,\mathrm{MC}}}, \tag{5.1}$$

with $K = B, C, D$. These leakage fractions are found to be small and are calculated in PYTHIA for the central value, with SHERPA used as a cross-check.

The two-dimensional sidebands method assumes that the two chosen variables are independent for the background. The isolation and identification criteria are chosen to minimise any such dependence, but any deviation from this assumption can be accounted for by using MC simulations to calculate the ratio:

$$R_{\mathrm{bkg}} = \frac{N_{\mathrm{bkg}}^{A,\mathrm{MC}} \cdot N_{\mathrm{bkg}}^{D,\mathrm{MC}}}{N_{\mathrm{bkg}}^{B,\mathrm{MC}} \cdot N_{\mathrm{bkg}}^{C,\mathrm{MC}}}, \tag{5.2}$$

where $N_{\mathrm{bkg}}^{K,\mathrm{MC}}$ are the number of background events in each of the regions $K = A, B, C, D$. For the central value the assumption, confirmed in a control region, that they are independent ($R_{\mathrm{bkg}} = 1$) is used; however, R_{bkg} is varied in section 7 to obtain the systematic uncertainty of any potential dependence.

The four sideband regions, signal leakage fractions and R_{bkg} are then used to solve for $N_{\mathrm{signal}}^{A,\mathrm{data}}$ via:

$$N_{\mathrm{signal}}^{A,\mathrm{data}} = N^{A,\mathrm{data}} - R_{\mathrm{bkg}} \cdot \left((N^{B,\mathrm{data}} - f^{B,\mathrm{MC}} N_{\mathrm{signal}}^{A,\mathrm{data}}) \cdot \frac{(N^{C,\mathrm{data}} - f^{C,\mathrm{MC}} N_{\mathrm{signal}}^{A,\mathrm{data}})}{(N^{D,\mathrm{data}} - f^{D,\mathrm{MC}} N_{\mathrm{signal}}^{A,\mathrm{data}})} \right). \tag{5.3}$$

This solution is used in the cross-section measurement via the signal purity, which is defined as:

$$P_{\text{signal}} = \frac{N_{\text{signal}}^{A,\text{data}}}{N^{A,\text{data}}}. \tag{5.4}$$

In all four η^γ regions, P_{signal} is found to rise with E_{T}^γ from 60% at 25 GeV to 100% at around 300 GeV. In the highest E_{T}^γ interval the method is inaccurate due to a lack of events in the background regions so here the central value of P_{signal} from the previous E_{T}^γ interval is used in the cross-section calculation.

Finally, after the above subtraction a remaining background of fake photons from electrons is accounted for. As in previous measurements, this is estimated using MC simulations, scaled to the measured integrated luminosity in data, of Z and W boson decays to electrons. Reconstructed photons from these simulations passing the selection of section 4 are counted if they are geometrically matched to a particle-level electron. The number of fake photons removed ($N_{e\to\gamma}$) is less than 0.2% of the remaining signal photons ($N^{\gamma,\text{data}}P_{\text{signal}}$) in all four η^γ regions and for most of the E_{T}^γ range — only reaching a maximum of 0.7% in some low E_{T}^γ intervals. As this is such a small effect no systematic uncertainty is assigned to this subtraction.

6 Cross section

The differential isolated prompt photon cross section as a function of E_{T}^γ (calculated in four $|\eta^\gamma|$ regions) includes elements described in the previous sections and takes the form:

$$\frac{\mathrm{d}\sigma}{\mathrm{d}E_{\text{T}}^\gamma} = \frac{1}{\int \mathcal{L}\mathrm{d}t(\Delta E_{\text{T}}^\gamma)} \cdot (N^{\gamma,\text{data}} \cdot P_{\text{signal}} - N_{e\to\gamma}) \cdot \frac{1}{\epsilon_{\text{trig}}} \cdot \frac{1}{\epsilon_{\text{corr}}}, \tag{6.1}$$

where E_{T}^γ is that of the highest transverse energy photon satisfying the kinematic, identification and isolation criteria (section 4). The trigger efficiency (ϵ_{trig}) corrects $N^{\gamma,\text{data}}$ for any events that would satisfy the selection criteria but were not recorded in the dataset (section 2). The number of events ($N^{\gamma,\text{data}}$) with a photon satisfying the selection criteria is corrected for background using the previously introduced subtraction factors P_{signal} and $N_{e\to\gamma}$ (section 5). Further, the overall size of the studied dataset is accounted for by dividing by the total integrated luminosity ($\int \mathcal{L}\mathrm{d}t$) and the cross section is normalised to inverse GeV by dividing each measured E_{T}^γ interval by its size ($\Delta E_{\text{T}}^\gamma$).

The remaining factor, ϵ_{corr}, is the unfolding correction factor used to correct the measurement to particle level to allow for direct comparisons to theoretical predictions. The unfolding factors are derived using PYTHIA, with SHERPA used as a cross-check. The unfolding correction factors are extracted by using a bin-by-bin unfolding procedure and are defined as:

$$\epsilon_{\text{corr}} = \frac{N_{\text{signal}}^{\text{MC}}}{N_{\text{particle}}^{\text{MC}}}, \tag{6.2}$$

where $N_{\text{signal}}^{\text{MC}}$ and $N_{\text{particle}}^{\text{MC}}$ refer to the number of events with an isolated photon at detector level and particle level respectively.

The main contribution to ϵ_{corr} is the identification efficiency (section 4.1), resulting in a very similar shape including the slight decrease at high E_{T}^{γ}. However, ϵ_{corr} differs as it also contains the effects from photon migrations between different E_{T}^{γ} intervals and the isolation efficiency (section 4.2). The overall correction lies between 0.8 and 0.9 and therefore indicates that detector effects are rather small.

The results of the bin-by-bin unfolding procedure are cross-checked using an iterative unfolding method, which reduces the reliance on the shape of the MC simulation distributions of E_{T}^{γ} at particle or detector level. The method is based on Bayes Theorem [54] and iteratively[6] unfolds the spectrum by changing the prior of the particle-level distribution to the previously unfolded spectrum for the next iteration. The results show that the two unfolding procedures are in very good agreement, considering statistical uncertainties only.

7   Uncertainties

To estimate the systematic uncertainties, the cross-section calculation was repeated varying the selection procedure, background subtraction techniques or the unfolding correction factor. One difference compared to the previous analyses is that this measurement makes use of the Bootstrap technique [55] to evaluate the statistical influence on systematic uncertainties, achieved by producing a large number of weighted (based on a Poisson distribution) replicas for each event. The result is then used to reduce the statistical fluctuations by applying a two-step smoothing technique; firstly combining E_{T}^{γ} intervals until the propagated uncertainty has a sufficiently large statistical significance, followed by performing a Gaussian kernel smoothing on the original E_{T}^{γ} intervals.

The following text describes the included uncertainty sources (quantifying those that are smaller):

- The photon energy scale is altered by varying systematic sources up and down, with the resulting shifts being summed in quadrature to provide the total uncertainty. The sources are split to account for correlations and range from being related to: detector material and read-out; simulation of the detector; extrapolations from data-driven measurements; and finally details related to the differences between unconverted or converted photon showers in the calorimeter. The uncertainty in the photon energy scale is around 1%, except for the region $1.56 \leq |\eta^{\gamma}| < 1.81$, but the uncertainty in the measurement is larger due to the steeply falling cross section.

- The admixture of direct and fragmentation photons in a given E_{T}^{γ} interval affects the calculation of both P_{signal} and ϵ_{corr}. Instead of using the default MC simulation fraction, a fit of the E_{T}^{γ} distribution is performed in PYTHIA to find the optimal admixture (as done in the recent photon plus jet paper [36]). The uncertainty is derived by comparing the results from this optimal admixture with the default PYTHIA simulation. This replaces the systematic uncertainty obtained previously from an arbitrary removal or doubling of the fragmentation component.

---

[6]In this analysis the result converges after four iterations.

- R_{bkg} is set to unity when P_{signal} is calculated. As described in section 5, this follows the assumption that there are no correlations between the isolation and identification criteria for the background. A test of this assumption is performed by subdividing the background-dominated region with an additional non-isolated criterion and then repeating the two-dimensional sidebands in background only regions. A 10% difference from unity is found in this test, which is then applied to R_{bkg} to calculate the uncertainty.

- As described in section 4.1, the photon identification efficiency in the MC simulations uses correction factors and the associated uncertainty in these alters the cross section by 0.5% for most of the E_T^γ range. In the lowest E_T^γ intervals it reaches 2% and above 550 GeV it ranges from 1% to 4% (increasing with η^γ).

- For the above photon identification correction factors an extra uncertainty is required, obtained from MC simulations, to account for a small difference in the photon isolation requirement applied in this analysis from that used for the measurement of the photon identification efficiency. This impacts the cross section by 0.5% but rises to 1% for the highest E_T^γ intervals.

- The orthogonal identification selection in section 5 relies on inverting the selection criteria of four of the shower-shape variables. The uncertainty in this procedure is estimated by inverting either only two of these variables or by inverting an extra variable. A data-driven technique is used to disentangle this uncertainty from that already included in the R_{bkg} uncertainty above. The resulting uncertainty is 2% for $E_T^\gamma < 100$ GeV but quickly falls to zero for higher E_T^γ.

- The isolation requirement used to define the background region in the P_{signal} calculation was altered so that the constant part of the requirement (7.8 GeV) was varied by ± 1 GeV (chosen as it is larger than any difference in the MC simulations between particle-level and detector-level isolation). The resulting uncertainty is less than 0.5%.

- The photon energy resolution is calculated from several independent sources in a similar manner to the energy scale, but the resolution is found to be of much less importance than the scale as it only produces an uncertainty of 0.5%, which rises to 1% for the highest E_T^γ intervals.

- The effect of unfolding is investigated by using a smooth function to reweight the MC simulations to match the data E_T^γ distribution. Unfolding the data using this reweighted MC prediction gives a difference of less than 0.5% compared to the nominal value.

- The uncertainty in the correction factors from the choice of QCD-cascade and hadronisation model is derived from comparing SHERPA with PYTHIA. To avoid double counting the effects from the fragmentation contribution, the PYTHIA simulation
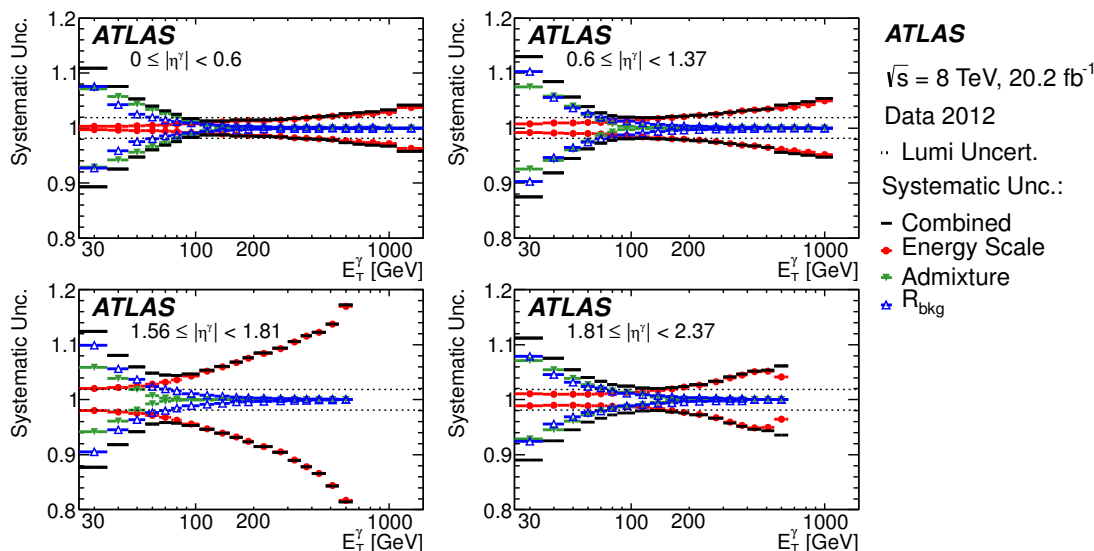
Figure 2. Summary of the relative size of the combined systematic uncertainty (which excludes the luminosity) and its four main contributions, shown as a function of E_T^γ.

with the optimal admixture of direct and fragmentation photons is used again. The resulting uncertainty is 2% at low E_T^γ but quickly falls to zero as E_T^γ increases.

- The integrated luminosity has an uncertainty measured to be $\pm 1.9\%$. It is derived, following the same methodology as that detailed in ref. [22], from a calibration of the luminosity scale derived from beam-separation scans performed in November 2012.

- Other uncertainties were studied, but are not included in the systematic uncertainty as they were found to be negligible. Examples of these studies include: investigating the trigger efficiency (statistical uncertainties are $< 0.1\%$), pile-up (splitting the dataset by number of interactions per bunch crossing) and the MC simulation isolation shift (correcting the MC simulation by twice the fit accuracy).

The systematic uncertainties except for the luminosity uncertainty are combined. This is done by treating each of the sources as uncorrelated in each E_T^γ interval. However, the sources are treated as correlated across different intervals in E_T^γ. This combination is shown in figure 2 along with several of the main systematic uncertainties detailed above. The energy scale uncertainty dominates the high-E_T^γ region, especially in the region $1.56 < |\eta^\gamma| < 1.81$. At low E_T^γ the uncertainties from the R_{bkg} variation and admixture of direct and fragmentation photons are of similar magnitude and dominate the uncertainty. In the E_T^γ range 80–200 GeV the main systematic uncertainties are of similar order and, in all but the region $1.56 < |\eta^\gamma| < 1.81$, this leads to the luminosity uncertainty being larger than this combination of the other systematic uncertainties.

The statistical uncertainty is mainly from the data, but also has a component due to the MC simulation. This component is from the reliance on MC simulations in the calculation of P_{signal} and ϵ_{corr}. The resulting total statistical uncertainty is 1–2% for most of the measured E_T^γ range, until it rises steeply in the highest E_T^γ intervals.
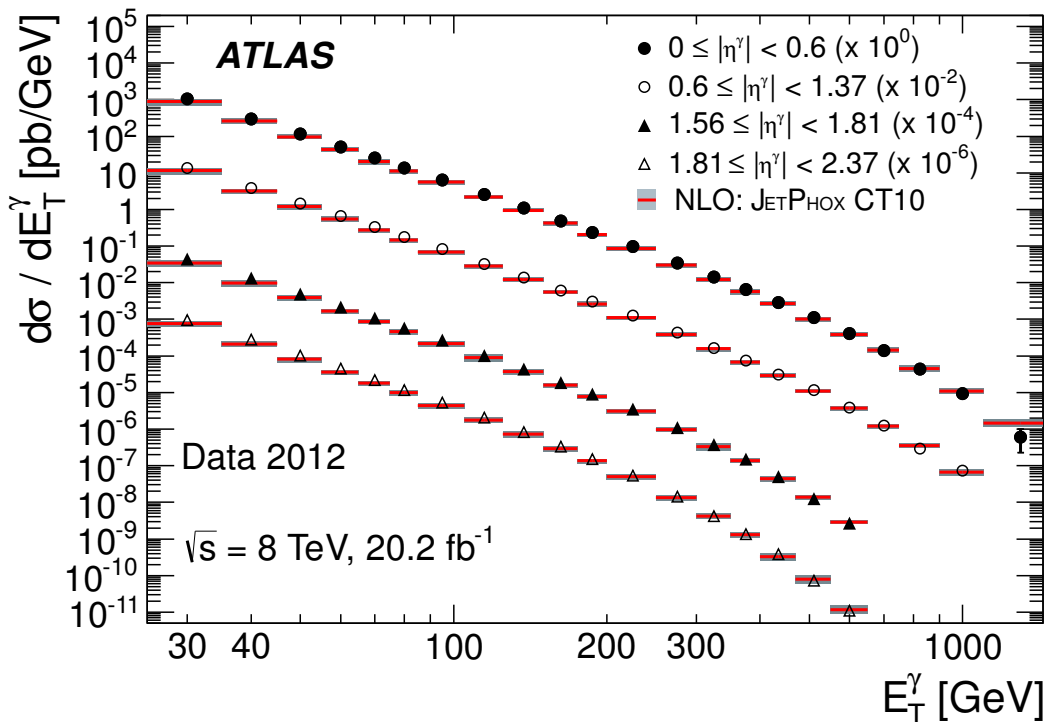
Figure 3. Differential cross sections from data and JETPHOX (using the CT10 PDF), shown as a function of E_T^γ for the four $|\eta^\gamma|$ regions. The distributions are scaled, by specified factors, to separate the distributions visually.

8 Results and discussion

The final cross sections are measured following eq. (6.1) in the fiducial region given in section 1. The systematic uncertainties, as described in section 7, are combined with the statistical uncertainty, but do not include the luminosity uncertainty. The measured cross sections are compared to theoretical predictions, as detailed in section 3, along with uncertainties from the combination of the scale, PDF, α_S and hadronisation plus UE uncertainties. Figure 3 shows a summary of the results (with the measured cross sections also being tabulated in appendix A), where it can be seen that the measurement is well described overall by JETPHOX over ten orders of magnitude in cross section. The total cross sections shown in table 1 are integrated over the entire E_T^γ for each η^γ region. As seen in the previous measurement [9] the total cross sections are 20% higher in data than those predicted by JETPHOX, but the results are consistent within the uncertainties. It can also be seen that the measurement uncertainty, dominated by the systematic uncertainty, is smaller than the theoretical uncertainty.

The difference between data and JETPHOX is explored further in figure 4 where the cross-section ratios are shown in each of the four η^γ regions as a function E_T^γ. Each η^γ region shows a similar trend at low E_T^γ, in that the JETPHOX NLO predictions are up to 20% lower than those measured. This difference remains constant, especially in the central η^γ region, for $E_T^\gamma < 500$ GeV where the fragmentation contribution decreases with E_T^γ from being

$|\eta^\gamma|$ range	E_T^γ range [GeV]	Measured total σ [nb]	JETPHOX total σ [nb]
0–0.6	25–1500	$15.6^{+1.4}_{-1.4}(\mathrm{syst}) \pm 0.02(\mathrm{stat}) \pm 0.3(\mathrm{lumi})$	$13.3 \pm 2.6(\mathrm{theory})$
0.6–1.37	25–1100	$20.2^{+2.2}_{-2.1}(\mathrm{syst}) \pm 0.03(\mathrm{stat}) \pm 0.4(\mathrm{lumi})$	$17.1 \pm 3.2(\mathrm{theory})$
1.56–1.81	25–650	$6.7^{+0.7}_{-0.7}(\mathrm{syst}) \pm 0.02(\mathrm{stat}) \pm 0.1(\mathrm{lumi})$	$5.2 \pm 1.0(\mathrm{theory})$
1.81–2.37	25–650	$14.3^{+1.4}_{-1.3}(\mathrm{syst}) \pm 0.03(\mathrm{stat}) \pm 0.3(\mathrm{lumi})$	$11.4 \pm 2.3(\mathrm{theory})$

Table 1. Measured and predicted total cross sections shown for each of the four $|\eta^\gamma|$ ranges. The JETPHOX predictions are made using the CT10 PDF.
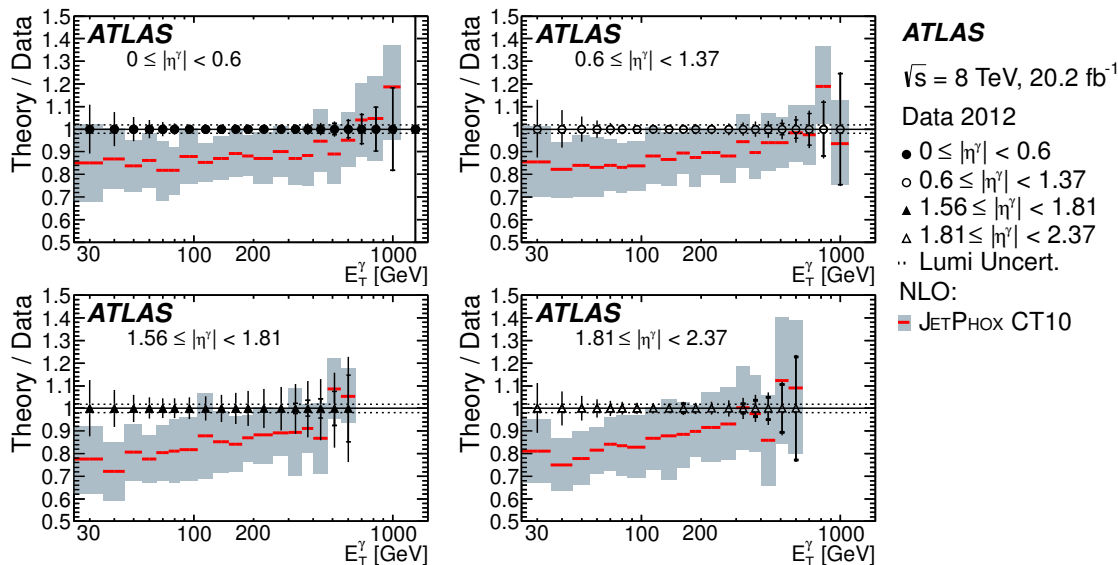

Figure 4. Ratio of theory (JETPHOX using the CT10 PDF) to data for the differential cross sections as a function of E_T^γ for the four $|\eta^\gamma|$ regions. The statistical component of the uncertainty in the data is indicated by the horizontal tick marks whereas the whole error bar corresponds to the combined statistical and systematic uncertainty (the additional systematic uncertainty arising from the uncertainty in the integrated luminosity is displayed separately as a dotted line). The NLO total uncertainty from JETPHOX is displayed as a band, which corresponds to the combination of the scale, α_S, PDF and hadronisation-plus-UE uncertainties. In the highest E_T^γ interval of the $|\eta^\gamma| < 0.6$ region the theoretical prediction and uncertainty is not shown as it is above the range of the figure.

a large contribution to the cross section, showing that JETPHOX models this contribution well apart from the normalisation. The normalisation difference decreases above this E_T^γ and in the range $1100 \leq E_\mathrm{T}^\gamma < 1500$ GeV the prediction overestimates the measurement, although this is where the experimental and PDF uncertainties are largest. The results are shown using the CT10 PDF, but there is very little difference when comparing the central value to those from MSTW2008, NNPDF2.3 and HeraPDF1.5, with any difference at high E_T^γ being covered by the large theoretical uncertainty.

The overall trend in differences between data and theory is similar to that seen in the measurement using 2011 data. However, a significant increase in the experimental

$|\eta^\gamma|$ range	E_{T}^γ range [GeV]	PETER total σ [nb]
0–0.6	25–1500	14.8 ± 2.0(theory)
0.6–1.37	25–1100	19.0 ± 2.5(theory)
1.56–1.81	25–650	5.7 ± 0.7(theory)
1.81–2.37	25–650	12.7 ± 1.8(theory)

Table 2. Predicted total cross sections from PETER shown for each of the four $|\eta^\gamma|$ ranges, made using the CT10 PDF.

precision of this measurement compared to the previous ATLAS measurements reveals new qualitative features in the comparison to JETPHOX. While the theoretical uncertainties have not changed, the measurement uncertainties are halved over most of the phase space.[7] This makes the uncertainties considerably smaller than the theoretical uncertainties, except in the statistically limited highest E_{T}^γ intervals, which leads to disagreement in some E_{T}^γ intervals between the measurement and the JETPHOX prediction. This improvement in accuracy can help to reduce PDF uncertainties once the measurement is included in a global fit.

In order for the data to provide a tighter constraint on proton PDF uncertainties, it would be preferable both to have a better general agreement between data and the predictions and also to reduce the dominant theoretical scale uncertainties. This can be achieved by using calculations beyond NLO, as done here by using the predictions from PETER. This comparison is shown in figure 5 where it can be seen that PETER does an excellent job of removing the normalisation difference seen between data and JETPHOX, especially in the region $|\eta^\gamma| < 1.37$. The uncertainties shown, from combining the scale, PDF and electroweak uncertainties, are about 20% lower than those from JETPHOX. The PETER predictions match the data well, within the combined measured and theoretical uncertainties, in all of the measured phase space. The improved normalisation and smaller uncertainties are also seen in the total cross sections as shown in table 2.

Finally, the measured cross sections are also compared to the LO parton shower MC calculations in figure 6. Here it can be seen that generally SHERPA, without any normalisation scaling, matches the data in the range $100 \le E_{\mathrm{T}}^\gamma < 500$ GeV in all four η^γ regions. At low E_{T}^γ, where a larger fragmentation contribution is expected, SHERPA matches the predictions from JETPHOX and thus is in disagreement with the measurement. At high E_{T}^γ the SHERPA prediction tends to be above the measured value. PYTHIA on the other hand is similar to JETPHOX for $E_{\mathrm{T}}^\gamma > 100$ GeV and hence is below the measured cross section in all η^γ regions except $1.81 \le |\eta^\gamma| < 2.37$. At low E_{T}^γ, the PYTHIA prediction has a very different shape than both the measurement and the other predictions, tending to overestimate the measured cross section, which suggests that the fragmentation contribution is not well modelled by the parton shower.

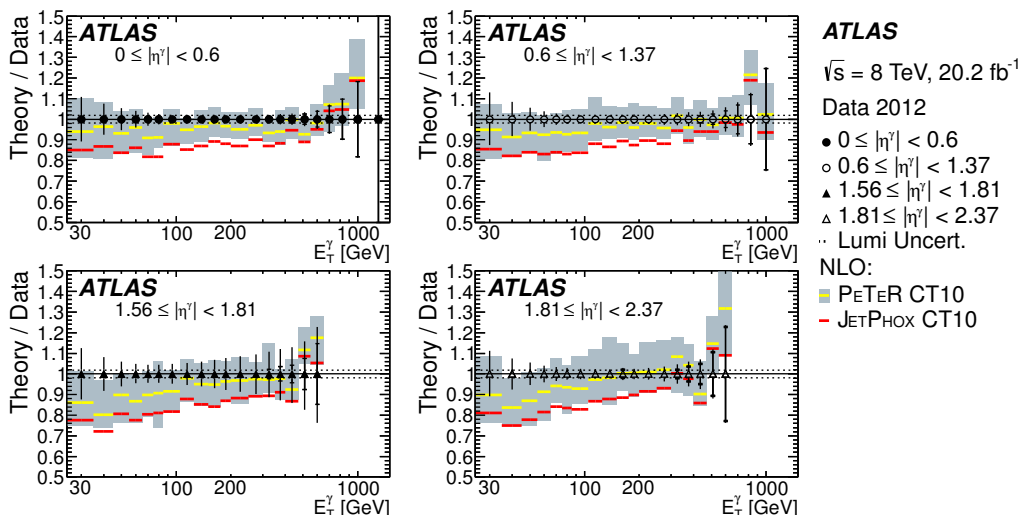[7]Only in the region $1.56 \le |\eta^\gamma| < 1.81$ is the 2011 uncertainty comparable, as it is measured in a larger η^γ region.

Figure 5. Ratio of theory (PᴇTᴇR and JᴇTPʜᴏx both using the CT10 PDF) to data for the differential cross sections as a function of E_T^γ for the four $|\eta^\gamma|$ regions. The statistical component of the uncertainty in the data is indicated by the horizontal tick marks whereas the whole error bar corresponds to the combined statistical and systematic uncertainty (the additional systematic uncertainty arising from the uncertainty in the integrated luminosity is displayed separately as a dotted line). The NLO total uncertainty from PᴇTᴇR is displayed as a band, which corresponds to the combination of the scale, PDF and electroweak uncertainties. In the highest E_T^γ interval of the $|\eta^\gamma| < 0.6$ region the theoretical predictions and uncertainty are not shown as they are above the range of the figure.

Figure 6. Ratio of theory (PʏTʜɪᴀ, Sʜᴇʀᴘᴀ and JᴇTPʜᴏx) to data for the differential cross sections as a function of E_T^γ for the four $|\eta^\gamma|$ regions. The statistical component of the uncertainty in the data is indicated by the horizontal tick marks whereas the whole error bar corresponds to the combined statistical and systematic uncertainty (the additional systematic uncertainty arising from the uncertainty in the integrated luminosity is displayed separately as a dotted line). The NLO total uncertainty from JᴇTPʜᴏx is displayed as a band, which corresponds to the combination of the scale, α_S, PDF and hadronisation-plus-UE uncertainties. In the highest E_T^γ interval of the $|\eta^\gamma| < 0.6$ region the theoretical predictions and uncertainty are not shown as they are above the range of the figure.

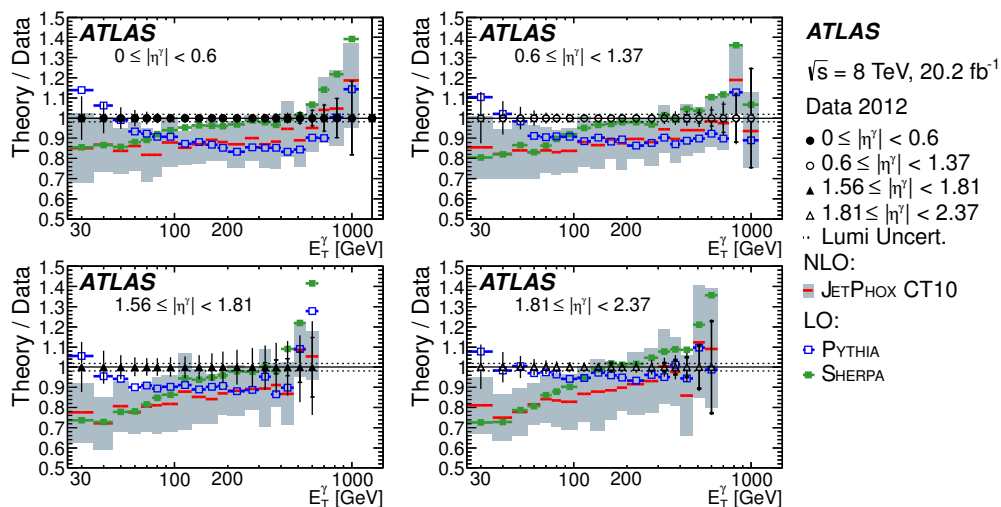## 9 Conclusion

In conclusion, a measurement of the inclusive isolated photon cross section has been presented, using 20.2 fb^{-1} of $\sqrt{s} = 8$ TeV proton-proton collision data recorded by the ATLAS detector at the LHC. This is measured for the highest-energy photon in the event, spanning $25 < E_{\mathrm{T}}^{\gamma} < 1500$ GeV, in one of four η^{γ} regions ($|\eta^{\gamma}| < 0.6$, $0.6 \leq |\eta^{\gamma}| < 1.37$, $1.56 \leq |\eta^{\gamma}| < 1.81$ and $1.81 \leq |\eta^{\gamma}| < 2.37$) and with the isolation requirement $E_{\mathrm{T}}^{\mathrm{iso}} < 4.8$ GeV $+ 4.2 \times 10^{-3} \times E_{\mathrm{T}}^{\gamma}$ calculated within a cone of size $\Delta R = 0.4$. The results presented cover ten orders of magnitude in cross section, extending the measurement above 1 TeV whilst also revisiting lower-E_{T}^{γ} data points. The results show a significant improvement in experimental uncertainties over the previous measurements. The results are compared to JetPhox predictions, which, for most of the E_{T}^{γ} range, have a similar shape but lie below the data. The predictions from PeTeR agree much better in normalisation and, unlike JetPhox, are within the uncertainties of the measured cross section for the entire phase space measured, showing the need for higher-order calculations to better understand this process theoretically. Comparing the results to LO parton shower MC calculations shows different trends, with the largest differences being at low E_{T}^{γ} in the region dominated by the fragmentation contribution. Finally, halving the measured uncertainties compared to previous measurements will make this a useful constraint on proton PDF uncertainties once the result is included in a global fit.

A Tables of measured cross sections

The measured E_{T}^{γ}-differential cross sections are listed in tables 3, 4, 5 and 6.

E_{T}^{γ} range [GeV]	$\mathrm{d}\sigma^{\gamma}/\mathrm{d}E_{\mathrm{T}}^{\gamma}$	Stat. Unc.	Sys. Unc.	Lumi. Unc.	[pb/GeV]
25–35	1.03	±0.00	$\pm_{0.11}^{0.11}$	±0.02	$\cdot 10^{3}$
35–45	3.01	±0.01	$\pm_{0.22}^{0.23}$	±0.06	$\cdot 10^{2}$
45–55	1.15	±0.01	$\pm_{0.06}^{0.06}$	±0.02	$\cdot 10^{2}$
55–65	5.03	±0.02	$\pm_{0.20}^{0.20}$	±0.10	$\cdot 10^{1}$
65–75	2.54	±0.01	$\pm_{0.08}^{0.08}$	±0.05	$\cdot 10^{1}$
75–85	1.37	±0.01	$\pm_{0.03}^{0.03}$	±0.03	$\cdot 10^{1}$
85–105	6.37	±0.03	$\pm_{0.11}^{0.11}$	±0.12	
105–125	2.54	±0.01	$\pm_{0.03}^{0.03}$	±0.05	
125–150	1.09	±0.00	$\pm_{0.01}^{0.01}$	±0.02	
150–175	4.84	±0.02	$\pm_{0.07}^{0.07}$	±0.09	$\cdot 10^{-1}$
175–200	2.34	±0.01	$\pm_{0.03}^{0.03}$	±0.04	$\cdot 10^{-1}$
200–250	9.84	±0.05	$\pm_{0.15}^{0.14}$	±0.19	$\cdot 10^{-2}$
250–300	3.42	±0.02	$\pm_{0.06}^{0.05}$	±0.07	$\cdot 10^{-2}$
300–350	1.41	±0.01	$\pm_{0.03}^{0.02}$	±0.03	$\cdot 10^{-2}$
350–400	6.56	±0.10	$\pm_{0.13}^{0.13}$	±0.13	$\cdot 10^{-3}$
400–470	2.84	±0.05	$\pm_{0.06}^{0.06}$	±0.05	$\cdot 10^{-3}$
470–550	1.13	±0.03	$\pm_{0.02}^{0.03}$	±0.02	$\cdot 10^{-3}$
550–650	4.05	±0.15	$\pm_{0.11}^{0.10}$	±0.08	$\cdot 10^{-4}$
650–750	1.39	±0.09	$\pm_{0.04}^{0.04}$	±0.03	$\cdot 10^{-4}$
750–900	4.36	±0.42	$\pm_{0.13}^{0.13}$	±0.08	$\cdot 10^{-5}$
900–1100	9.35	±1.71	$\pm_{0.31}^{0.31}$	±0.18	$\cdot 10^{-6}$
1100–1500	6.12	±3.80	$\pm_{0.26}^{0.25}$	±0.12	$\cdot 10^{-7}$

Table 3. The inclusive prompt photon cross section with systematic and statistical uncertainties for the region $|\eta^{\gamma}| < 0.6$.

E_T^γ range [GeV]	$\mathrm{d}\sigma^\gamma/\mathrm{d}E_T^\gamma$	Stat. Unc.	Sys. Unc.	Lumi. Unc.	[pb/GeV]
25–35	1.34	±0.00	$\pm^{0.17}_{0.17}$	±0.03	$\cdot 10^3$
35–45	3.88	±0.01	$\pm^{0.33}_{0.31}$	±0.07	$\cdot 10^2$
45–55	1.44	±0.01	$\pm^{0.08}_{0.08}$	±0.03	$\cdot 10^2$
55–65	6.61	±0.03	$\pm^{0.25}_{0.25}$	±0.13	$\cdot 10^1$
65–75	3.30	±0.01	$\pm^{0.09}_{0.09}$	±0.06	$\cdot 10^1$
75–85	1.77	±0.01	$\pm^{0.04}_{0.04}$	±0.03	$\cdot 10^1$
85–105	8.20	±0.03	$\pm^{0.16}_{0.16}$	±0.16	
105–125	3.24	±0.01	$\pm^{0.06}_{0.06}$	±0.06	
125–150	1.39	±0.00	$\pm^{0.03}_{0.03}$	±0.03	
150–175	6.16	±0.02	$\pm^{0.13}_{0.13}$	±0.12	$\cdot 10^{-1}$
175–200	3.01	±0.02	$\pm^{0.07}_{0.06}$	±0.06	$\cdot 10^{-1}$
200–250	1.25	±0.05	$\pm^{0.03}_{0.03}$	±0.02	$\cdot 10^{-1}$
250–300	4.31	±0.03	$\pm^{0.11}_{0.11}$	±0.08	$\cdot 10^{-2}$
300–350	1.66	±0.02	$\pm^{0.05}_{0.05}$	±0.03	$\cdot 10^{-2}$
350–400	7.56	±0.11	$\pm^{0.23}_{0.23}$	±0.14	$\cdot 10^{-3}$
400–470	3.08	±0.05	$\pm^{0.10}_{0.10}$	±0.06	$\cdot 10^{-3}$
470–550	1.16	±0.03	$\pm^{0.04}_{0.04}$	±0.02	$\cdot 10^{-3}$
550–650	3.82	±0.15	$\pm^{0.16}_{0.17}$	±0.07	$\cdot 10^{-4}$
650–750	1.24	±0.09	$\pm^{0.05}_{0.06}$	±0.02	$\cdot 10^{-4}$
750–900	2.96	±0.35	$\pm^{0.14}_{0.14}$	±0.06	$\cdot 10^{-5}$
900–1100	7.23	±1.78	$\pm^{0.39}_{0.38}$	±0.14	$\cdot 10^{-6}$

Table 4. The inclusive prompt photon cross section with systematic and statistical uncertainties for the region $0.6 \leq |\eta^\gamma| < 1.37$

E_T^γ range [GeV]	$d\sigma^\gamma/dE_T^\gamma$	Stat. Unc.	Sys. Unc.	Lumi. Unc.	[pb/GeV]
25–35	4.42	±0.02	$\pm_{0.54}^{0.55}$	±0.08	$\cdot 10^2$
35–45	1.34	±0.01	$\pm_{0.11}^{0.11}$	±0.03	$\cdot 10^2$
45–55	4.82	±0.05	$\pm_{0.28}^{0.29}$	±0.09	$\cdot 10^1$
55–65	2.15	±0.02	$\pm_{0.10}^{0.10}$	±0.04	$\cdot 10^1$
65–75	1.07	±0.01	$\pm_{0.04}^{0.05}$	±0.02	$\cdot 10^1$
75–85	5.77	±0.06	$\pm_{0.25}^{0.25}$	±0.11	
85–105	2.69	±0.02	$\pm_{0.13}^{0.13}$	±0.05	
105-125	1.02	±0.01	$\pm_{0.05}^{0.05}$	±0.02	
125–150	4.38	±0.02	$\pm_{0.27}^{0.26}$	±0.08	$\cdot 10^{-1}$
150–175	1.89	±0.01	$\pm_{0.13}^{0.13}$	±0.04	$\cdot 10^{-1}$
175–200	8.98	±0.10	$\pm_{0.69}^{0.69}$	±0.17	$\cdot 10^{-2}$
200–250	3.48	±0.03	$\pm_{0.30}^{0.29}$	±0.07	$\cdot 10^{-2}$
250–300	1.09	±0.01	$\pm_{0.10}^{0.10}$	±0.02	$\cdot 10^{-2}$
300–350	3.76	±0.08	$\pm_{0.41}^{0.40}$	±0.07	$\cdot 10^{-3}$
350–400	1.52	±0.05	$\pm_{0.19}^{0.18}$	±0.03	$\cdot 10^{-3}$
400–470	5.11	±0.22	$\pm_{0.69}^{0.63}$	±0.10	$\cdot 10^{-4}$
470–550	1.27	±0.10	$\pm_{0.20}^{0.18}$	±0.02	$\cdot 10^{-4}$
550–650	2.71	±0.40	$\pm_{0.50}^{0.47}$	±0.05	$\cdot 10^{-5}$

Table 5. The inclusive prompt photon cross section with systematic and statistical uncertainties for the region $1.56 \leq |\eta^\gamma| < 1.81$.

E_{T}^{γ} range [GeV]	$\mathrm{d}\sigma^{\gamma}/\mathrm{d}E_{\mathrm{T}}^{\gamma}$	Stat. Unc.	Sys. Unc.	Lumi. Unc.	[pb/GeV]
25–35	9.47	± 0.02	$\pm^{1.06}_{1.03}$	± 0.18	$\cdot 10^2$
35–45	2.84	± 0.01	$\pm^{0.21}_{0.21}$	± 0.05	$\cdot 10^2$
45–55	1.04	± 0.01	$\pm^{0.06}_{0.06}$	± 0.02	$\cdot 10^2$
55–65	4.48	± 0.02	$\pm^{0.18}_{0.18}$	± 0.09	$\cdot 10^1$
65–75	2.16	± 0.01	$\pm^{0.07}_{0.07}$	± 0.04	$\cdot 10^1$
75–85	1.18	± 0.01	$\pm^{0.03}_{0.03}$	± 0.02	$\cdot 10^1$
85–105	5.37	± 0.03	$\pm^{0.13}_{0.13}$	± 0.10	
105–125	2.05	± 0.01	$\pm^{0.04}_{0.04}$	± 0.04	
125–150	8.29	± 0.03	$\pm^{0.17}_{0.17}$	± 0.16	$\cdot 10^{-1}$
150–175	3.32	± 0.07	$\pm^{0.07}_{0.07}$	± 0.06	$\cdot 10^{-1}$
175–200	1.52	± 0.01	$\pm^{0.04}_{0.04}$	± 0.03	$\cdot 10^{-1}$
200–250	5.41	± 0.03	$\pm^{0.15}_{0.15}$	± 0.10	$\cdot 10^{-2}$
250–300	1.42	± 0.02	$\pm^{0.05}_{0.05}$	± 0.03	$\cdot 10^{-2}$
300–350	4.18	± 0.09	$\pm^{0.17}_{0.18}$	± 0.08	$\cdot 10^{-3}$
350–400	1.35	± 0.05	$\pm^{0.06}_{0.07}$	± 0.03	$\cdot 10^{-3}$
400–470	3.87	± 0.19	$\pm^{0.20}_{0.21}$	± 0.07	$\cdot 10^{-4}$
470–550	7.17	± 0.76	$\pm^{0.38}_{0.40}$	± 0.14	$\cdot 10^{-5}$
550–650	1.08	± 0.25	$\pm^{0.07}_{0.07}$	± 0.02	$\cdot 10^{-5}$

Table 6. The inclusive prompt photon cross section with systematic and statistical uncertainties for the region $1.82 \leq |\eta^{\gamma}| < 2.37$.

References

[1] P. Aurenche et al., *The gluon contents of the nucleon probed with real and virtual photons*, *Phys. Rev.* **D 39** (1989) 3275.

[2] H.L. Lai et al., *Global QCD analysis and the CTEQ parton distributions*, *Phys. Rev.* **D 51** (1995) 4763 [`hep-ph/9410404`] [INSPIRE].

[3] A.D. Martin, R.G. Roberts, W.J. Stirling and R.S. Thorne, *Parton distributions: a new global analysis*, *Eur. Phys. J.* **C 4** (1998) 463 [`hep-ph/9803445`] [INSPIRE].

[4] A.D. Martin, R.G. Roberts, W.J. Stirling and R.S. Thorne, *Parton distributions and the LHC: W and Z production*, *Eur. Phys. J.* **C 14** (2000) 133 [`hep-ph/9907231`] [INSPIRE].

[5] P. Aurenche, M. Fontannaz, J.-P. Guillet, E. Pilon and M. Werlen, *A new critical study of photon production in hadronic collisions*, *Phys. Rev.* **D 73** (2006) 094007 [hep-ph/0602133] [INSPIRE].

[6] D. d'Enterria and J. Rojo, *Quantitative constraints on the gluon distribution function in the proton from collider isolated-photon data*, *Nucl. Phys.* **B 860** (2012) 311 [arXiv:1202.1762] [INSPIRE].

[7] ATLAS collaboration, *Measurement of the inclusive isolated prompt photon cross section in pp collisions at $\sqrt{s} = 7$ TeV with the ATLAS detector*, *Phys. Rev.* **D 83** (2011) 052005 [arXiv:1012.4389] [INSPIRE].

[8] ATLAS collaboration, *Measurement of the inclusive isolated prompt photon cross-section in pp collisions at $\sqrt{s} = 7$ TeV using 35 pb^{-1} of ATLAS data*, *Phys. Lett.* **B 706** (2011) 150 [arXiv:1108.0253] [INSPIRE].

[9] ATLAS collaboration, *Measurement of the inclusive isolated prompt photons cross section in pp collisions at $\sqrt{s} = 7$ TeV with the ATLAS detector using $4.6\,fb^{-1}$*, *Phys. Rev.* **D 89** (2014) 052004 [arXiv:1311.1440] [INSPIRE].

[10] CMS collaboration, *Measurement of the isolated prompt photon production cross section in pp collisions at $\sqrt{s} = 7$ TeV*, *Phys. Rev. Lett.* **106** (2011) 082001 [arXiv:1012.0799] [INSPIRE].

[11] CMS collaboration, *Measurement of the differential cross section for isolated prompt photon production in pp collisions at 7 TeV*, *Phys. Rev.* **D 84** (2011) 052011 [arXiv:1108.2044] [INSPIRE].

[12] CDF collaboration, T. Aaltonen et al., *Measurement of the inclusive isolated prompt photon cross section in p$\bar{p}$ collisions at $\sqrt{s} = 1.96$ TeV using the CDF detector*, *Phys. Rev.* **D 80** (2009) 111106 [arXiv:0910.3623] [INSPIRE].

[13] D0 collaboration, V.M. Abazov et al., *Measurement of the differential cross sections for isolated direct photon pair production in p$\bar{p}$ collisions at $\sqrt{s} = 1.96$ TeV*, *Phys. Lett.* **B 725** (2013) 6 [arXiv:1301.4536] [INSPIRE].

[14] D0 collaboration, V.M. Abazov et al., *Measurement of the isolated photon cross section in p$\bar{p}$ collisions at $\sqrt{s} = 1.96$ TeV*, *Phys. Lett.* **B 639** (2006) 151 [*Erratum ibid.* **B 658** (2008) 285] [hep-ex/0511054] [INSPIRE].

[15] UA1 collaboration, C. Albajar et al., *Direct photon production at the CERN proton-anti-proton collider*, *Phys. Lett.* **B 209** (1988) 385.

[16] UA2 collaboration, J. Alitti et al., *A measurement of the direct photon production cross-section at the CERN $\bar{p}p$ collider*, *Phys. Lett.* **B 263** (1991) 544.

[17] H1 collaboration, F.D. Aaron et al., *Measurement of isolated photon production in deep-inelastic scattering at HERA*, *Eur. Phys. J.* **C 54** (2008) 371 [arXiv:0711.4578] [INSPIRE].

[18] ZEUS collaboration, S. Chekanov et al., *Measurement of isolated photon production in deep inelastic ep scattering*, *Phys. Lett.* **B 687** (2010) 16 [arXiv:0909.4223] [INSPIRE].

[19] H1 collaboration, F.D. Aaron et al., *Prompt photons in photoproduction at HERA*, *Eur. Phys. J.* **C 66** (2010) 17 [arXiv:0910.5631] [INSPIRE].

[20] ZEUS collaboration, H. Abramowicz et al., *Photoproduction of isolated photons, inclusively and with a jet, at HERA*, *Phys. Lett.* **B 730** (2014) 293 [arXiv:1312.1539] [INSPIRE].

[21] ATLAS collaboration, *The ATLAS experiment at the CERN Large Hadron Collider*, 2008 *JINST* **3** S08003.

[22] ATLAS collaboration, *Improved luminosity determination in pp collisions at $\sqrt{s} = 7$ TeV using the ATLAS detector at the LHC*, *Eur. Phys. J.* **C 73** (2013) 2518 [arXiv:1302.4393] [INSPIRE].

[23] ATLAS collaboration, *Performance of the ATLAS electron and photon trigger in pp collisions at $\sqrt{s} = 7$ TeV in 2011*, ATLAS-CONF-2012-048 (2012).

[24] T. Sjöstrand, S. Mrenna and P.Z. Skands, *A brief introduction to PYTHIA* 8.1, *Comput. Phys. Commun.* **178** (2008) 852 [arXiv:0710.3820] [INSPIRE].

[25] T. Gleisberg et al., *Event generation with SHERPA 1.1*, *JHEP* **02** (2009) 007 [arXiv:0811.4622] [INSPIRE].

[26] ATLAS collaboration, *The ATLAS simulation infrastructure*, *Eur. Phys. J.* **C 70** (2010) 823 [arXiv:1005.4568] [INSPIRE].

[27] S. Agostinelli et al., *GEANT4: a simulation toolkit*, *Nucl. Instrum. Meth.* **A 506** (2003) 250.

[28] S. Catani, M. Fontannaz, J.P. Guillet and E. Pilon, *Cross-section of isolated prompt photons in hadron hadron collisions*, *JHEP* **05** (2002) 028 [hep-ph/0204023] [INSPIRE].

[29] T. Becher, C. Lorentzen and M.D. Schwartz, *Precision direct photon and W-boson spectra at high p_T and comparison to LHC data*, *Phys. Rev.* **D 86** (2012) 054026 [arXiv:1206.6115] [INSPIRE].

[30] M.D. Schwartz, *Precision direct photon spectra at high energy and comparison to the 8 TeV ATLAS data*, arXiv:1606.02313 [INSPIRE].

[31] J.M. Campbell and R.K. Ellis, *MCFM for the Tevatron and the LHC*, *Nucl. Phys. Proc. Suppl.* **205-206** (2010) 10 [arXiv:1007.3492] [INSPIRE].

[32] J. Pumplin et al., *New generation of parton distributions with uncertainties from global QCD analysis*, *JHEP* **07** (2002) 012 [hep-ph/0201195] [INSPIRE].

[33] ATLAS collaboration, *Summary of ATLAS PYTHIA 8 tunes*, ATL-PHYS-PUB-2012-003 (2012).

[34] P. Bartalini et al., *Multi-parton interactions at the LHC*, arXiv:1111.0469 [INSPIRE].

[35] B. Andersson et al., *Parton fragmentation and string dynamics*, *Phys. Rept.* **97** (1983) 31.

[36] ATLAS collaboration, *Dynamics of isolated-photon plus jet production in pp collisions at $\sqrt{s} = 7$ TeV with the ATLAS detector*, *Nucl. Phys.* **B 875** (2013) 483 [arXiv:1307.6795] [INSPIRE].

[37] H.-L. Lai et al., *New parton distributions for collider physics*, *Phys. Rev.* **D 82** (2010) 074024 [arXiv:1007.2241] [INSPIRE].

[38] J.-C. Winter, F. Krauss and G. Soff, *A modified cluster hadronization model*, *Eur. Phys. J.* **C 36** (2004) 381 [hep-ph/0311085] [INSPIRE].

[39] L. Bourhis, M. Fontannaz and J.P. Guillet, *Quarks and gluon fragmentation functions into photons*, *Eur. Phys. J.* **C 2** (1998) 529 [hep-ph/9704447] [INSPIRE].

[40] L. Bourhis, M. Fontannaz, J.P. Guillet and M. Werlen, *Next-to-leading order determination of fragmentation functions*, *Eur. Phys. J.* **C 19** (2001) 89 [hep-ph/0009101] [INSPIRE].

[41] A.D. Martin, W.J. Stirling, R.S. Thorne and G. Watt, *Parton distributions for the LHC*, *Eur. Phys. J.* **C 63** (2009) 189 [arXiv:0901.0002] [INSPIRE].

[42] R.D. Ball et al., *Parton distributions with LHC data*, *Nucl. Phys.* **B 867** (2013) 244 [arXiv:1207.1303] [INSPIRE].

[43] H1 and ZEUS collaborations, *Combined results*, preliminary H1prelim-10-142, ZEUS-prel-10-018.

[44] W. Giele et al., *The QCD/SM working group: summary report*, hep-ph/0204316 [INSPIRE].

[45] R. Blair et al., *NLO theoretical predictions for photon measurements using the PHOX generators*, CERN-OPEN-2011-041 (2011).

[46] T. Becher and X. Garcia i Tormo, *Electroweak sudakov effects in W, Z and γ production at large transverse momentum*, *Phys. Rev.* **D 88** (2013) 013009 [arXiv:1305.4202] [INSPIRE].

[47] T. Becher and X. Garcia i Tormo, *Addendum: electroweak Sudakov effects in W, Z and γ production at large transverse momentum*, *Phys. Rev.* **D 92** (2015) 073011 [arXiv:1509.01961] [INSPIRE].

[48] T. Becher and M.D. Schwartz, *Direct photon production with effective field theory*, *JHEP* **02** (2010) 040 [arXiv:0911.0681] [INSPIRE].

[49] ATLAS collaboration, *A study of the sensitivity to the proton parton distributions of the inclusive photon production cross section in pp collisions at 7 TeV measured by the ATLAS experiment at the LHC*, ATL-PHYS-PUB-2013-018 (2013).

[50] ATLAS collaboration, *Measurement of the photon identification efficiencies with the ATLAS detector using LHC Run-1 data*, arXiv:1606.01813 [INSPIRE].

[51] ATLAS collaboration, *Expected photon performance in the ATLAS experiment*, ATL-PHYS-PUB-2011-007 (2011).

[52] ATLAS collaboration, *Electron and photon energy calibration with the ATLAS detector using LHC Run 1 data*, *Eur. Phys. J.* **C 74** (2014) 3071 [arXiv:1407.5063] [INSPIRE].

[53] M. Cacciari, G.P. Salam and S. Sapeta, *On the characterisation of the underlying event*, *JHEP* **04** (2010) 065 [arXiv:0912.4926] [INSPIRE].

[54] T. Bayes, *An essay toward solving a problem in the doctrine of chances*, *Phil. Trans. Roy. Soc. Lond.* **53** (1764) 370.

[55] G. Bohm, *Introduction to statistics and data analysis for physicists*, Verl. Dt. Elektronen-Synchrotron, Hamburg, Germany (2010), p. 336 [ISBN:978-3-935702-41-6].

The ATLAS collaboration

G. Aad[87], B. Abbott[114], J. Abdallah[65], O. Abdinov[12], B. Abeloos[118], R. Aben[108], M. Abolins[92],
O.S. AbouZeid[138], N.L. Abraham[150], H. Abramowicz[154], H. Abreu[153], R. Abreu[117],
Y. Abulaiti[147a,147b], B.S. Acharya[164a,164b,a], L. Adamczyk[40a], D.L. Adams[27], J. Adelman[109],
S. Adomeit[101], T. Adye[132], A.A. Affolder[76], T. Agatonovic-Jovin[14], J. Agricola[56],
J.A. Aguilar-Saavedra[127a,127f], S.P. Ahlen[24], F. Ahmadov[67,b], G. Aielli[134a,134b],
H. Akerstedt[147a,147b], T.P.A. Åkesson[83], A.V. Akimov[97], G.L. Alberghi[22a,22b], J. Albert[169],
S. Albrand[57], M.J. Alconada Verzini[73], M. Aleksa[32], I.N. Aleksandrov[67], C. Alexa[28b],
G. Alexander[154], T. Alexopoulos[10], M. Alhroob[114], M. Aliev[75a,75b], G. Alimonti[93a], J. Alison[33],
S.P. Alkire[37], B.M.M. Allbrooke[150], B.W. Allen[117], P.P. Allport[19], A. Aloisio[105a,105b],
A. Alonso[38], F. Alonso[73], C. Alpigiani[139], B. Alvarez Gonzalez[32], D. Álvarez Piqueras[167],
M.G. Alviggi[105a,105b], B.T. Amadio[16], K. Amako[68], Y. Amaral Coutinho[26a], C. Amelung[25],
D. Amidei[91], S.P. Amor Dos Santos[127a,127c], A. Amorim[127a,127b], S. Amoroso[32], N. Amram[154],
G. Amundsen[25], C. Anastopoulos[140], L.S. Ancu[51], N. Andari[109], T. Andeen[11], C.F. Anders[60b],
G. Anders[32], J.K. Anders[76], K.J. Anderson[33], A. Andreazza[93a,93b], V. Andrei[60a], S. Angelidakis[9],
I. Angelozzi[108], P. Anger[46], A. Angerami[37], F. Anghinolfi[32], A.V. Anisenkov[110,c], N. Anjos[13],
A. Annovi[125a,125b], M. Antonelli[49], A. Antonov[99], J. Antos[145b], F. Anulli[133a], M. Aoki[68],
L. Aperio Bella[19], G. Arabidze[92], Y. Arai[68], J.P. Araque[127a], A.T.H. Arce[47], F.A. Arduh[73],
J-F. Arguin[96], S. Argyropoulos[65], M. Arik[20a], A.J. Armbruster[32], L.J. Armitage[78], O. Arnaez[32],
H. Arnold[50], M. Arratia[30], O. Arslan[23], A. Artamonov[98], G. Artoni[121], S. Artz[85], S. Asai[156],
N. Asbah[44], A. Ashkenazi[154], B. Åsman[147a,147b], L. Asquith[150], K. Assamagan[27], R. Astalos[145a],
M. Atkinson[166], N.B. Atlay[142], K. Augsten[129], G. Avolio[32], B. Axen[16], M.K. Ayoub[118],
G. Azuelos[96,d], M.A. Baak[32], A.E. Baas[60a], M.J. Baca[19], H. Bachacou[137], K. Bachas[75a,75b],
M. Backes[32], M. Backhaus[32], P. Bagiacchi[133a,133b], P. Bagnaia[133a,133b], Y. Bai[35a], J.T. Baines[132],
O.K. Baker[176], E.M. Baldin[110,c], P. Balek[130], T. Balestri[149], F. Balli[137], W.K. Balunas[123],
E. Banas[41], Sw. Banerjee[173,e], A.A.E. Bannoura[175], L. Barak[32], E.L. Barberio[90],
D. Barberis[52a,52b], M. Barbero[87], T. Barillari[102], T. Barklow[144], N. Barlow[30], S.L. Barnes[86],
B.M. Barnett[132], R.M. Barnett[16], Z. Barnovska[5], A. Baroncelli[135a], G. Barone[25], A.J. Barr[121],
L. Barranco Navarro[167], F. Barreiro[84], J. Barreiro Guimarães da Costa[35a], R. Bartoldus[144],
A.E. Barton[74], P. Bartos[145a], A. Basalaev[124], A. Bassalat[118], A. Basye[166], R.L. Bates[55],
S.J. Batista[159], J.R. Batley[30], M. Battaglia[138], M. Bauce[133a,133b], F. Bauer[137], H.S. Bawa[144,f],
J.B. Beacham[112], M.D. Beattie[74], T. Beau[82], P.H. Beauchemin[162], P. Bechtle[23], H.P. Beck[18,g],
K. Becker[121], M. Becker[85], M. Beckingham[170], C. Becot[111], A.J. Beddall[20e], A. Beddall[20b],
V.A. Bednyakov[67], M. Bedognetti[108], C.P. Bee[149], L.J. Beemster[108], T.A. Beermann[32],
M. Begel[27], J.K. Behr[44], C. Belanger-Champagne[89], A.S. Bell[80], G. Bella[154], L. Bellagamba[22a],
A. Bellerive[31], M. Bellomo[88], K. Belotskiy[99], O. Beltramello[32], N.L. Belyaev[99], O. Benary[154],
D. Benchekroun[136a], M. Bender[101], K. Bendtz[147a,147b], N. Benekos[10], Y. Benhammou[154],
E. Benhar Noccioli[176], J. Benitez[65], J.A. Benitez Garcia[160b], D.P. Benjamin[47], J.R. Bensinger[25],
S. Bentvelsen[108], L. Beresford[121], M. Beretta[49], D. Berge[108], E. Bergeaas Kuutmann[165],
N. Berger[5], F. Berghaus[169], J. Beringer[16], S. Berlendis[57], N.R. Bernard[88], C. Bernius[111],
F.U. Bernlochner[23], T. Berry[79], P. Berta[130], C. Bertella[85], G. Bertoli[147a,147b],
F. Bertolucci[125a,125b], I.A. Bertram[74], C. Bertsche[114], D. Bertsche[114], G.J. Besjes[38],
O. Bessidskaia Bylund[147a,147b], M. Bessner[44], N. Besson[137], C. Betancourt[50], S. Bethke[102],
A.J. Bevan[78], W. Bhimji[16], R.M. Bianchi[126], L. Bianchini[25], M. Bianco[32], O. Biebel[101],
D. Biedermann[17], R. Bielski[86], N.V. Biesuz[125a,125b], M. Biglietti[135a], J. Bilbao De Mendizabal[51],
H. Bilokon[49], M. Bindi[56], S. Binet[118], A. Bingul[20b], C. Bini[133a,133b], S. Biondi[22a,22b],
D.M. Bjergaard[47], C.W. Black[151], J.E. Black[144], K.M. Black[24], D. Blackburn[139], R.E. Blair[6],
J.-B. Blanchard[137], J.E. Blanco[79], T. Blazek[145a], I. Bloch[44], C. Blocker[25], W. Blum[85,*],
U. Blumenschein[56], S. Blunier[34a], G.J. Bobbink[108], V.S. Bobrovnikov[110,c], S.S. Bocchetta[83],
A. Bocci[47], C. Bock[101], M. Boehler[50], D. Boerner[175], J.A. Bogaerts[32], D. Bogavac[14],
A.G. Bogdanchikov[110], C. Bohm[147a], V. Boisvert[79], T. Bold[40a], V. Boldea[28b],
A.S. Boldyrev[164a,164c], M. Bomben[82], M. Bona[78], M. Boonekamp[137], A. Borisov[131], G. Borissov[74],

J. Bortfeldt[101], D. Bortoletto[121], V. Bortolotto[62a,62b,62c], K. Bos[108], D. Boscherini[22a],
M. Bosman[13], J.D. Bossio Sola[29], J. Boudreau[126], J. Bouffard[2], E.V. Bouhova-Thacker[74],
D. Boumediene[36], C. Bourdarios[118], S.K. Boutle[55], A. Boveia[32], J. Boyd[32], I.R. Boyko[67],
J. Bracinik[19], A. Brandt[8], G. Brandt[56], O. Brandt[60a], U. Bratzler[157], B. Brau[88], J.E. Brau[117],
H.M. Braun[175,*], W.D. Breaden Madden[55], K. Brendlinger[123], A.J. Brennan[90], L. Brenner[108],
R. Brenner[165], S. Bressler[172], T.M. Bristow[48], D. Britton[55], D. Britzger[44], F.M. Brochu[30],
I. Brock[23], R. Brock[92], G. Brooijmans[37], T. Brooks[79], W.K. Brooks[34b], J. Brosamer[16],
E. Brost[117], J.H Broughton[19], P.A. Bruckman de Renstrom[41], D. Bruncko[145b], R. Bruneliere[50],
A. Bruni[22a], G. Bruni[22a], BH Brunt[30], M. Bruschi[22a], N. Bruscino[23], P. Bryant[33],
L. Bryngemark[83], T. Buanes[15], Q. Buat[143], P. Buchholz[142], A.G. Buckley[55], I.A. Budagov[67],
F. Buehrer[50], M.K. Bugge[120], O. Bulekov[99], D. Bullock[8], H. Burckhart[32], S. Burdin[76],
C.D. Burgard[50], B. Burghgrave[109], K. Burka[41], S. Burke[132], I. Burmeister[45], E. Busato[36],
D. Büscher[50], V. Büscher[85], P. Bussey[55], J.M. Butler[24], A.I. Butt[3], C.M. Buttar[55],
J.M. Butterworth[80], P. Butti[108], W. Buttinger[27], A. Buzatu[55], A.R. Buzykaev[110,c],
S. Cabrera Urbán[167], D. Caforio[129], V.M. Cairo[39a,39b], O. Cakir[4a], N. Calace[51], P. Calafiura[16],
A. Calandri[87], G. Calderini[82], P. Calfayan[101], L.P. Caloba[26a], D. Calvet[36], S. Calvet[36],
T.P. Calvet[87], R. Camacho Toro[33], S. Camarda[32], P. Camarri[134a,134b], D. Cameron[120],
R. Caminal Armadans[166], C. Camincher[57], S. Campana[32], M. Campanelli[80], A. Campoverde[149],
V. Canale[105a,105b], A. Canepa[160a], M. Cano Bret[35e], J. Cantero[84], R. Cantrill[127a], T. Cao[42],
M.D.M. Capeans Garrido[32], I. Caprini[28b], M. Caprini[28b], M. Capua[39a,39b], R. Caputo[85],
R.M. Carbone[37], R. Cardarelli[134a], F. Cardillo[50], I. Carli[130], T. Carli[32], G. Carlino[105a],
L. Carminati[93a,93b], S. Caron[107], E. Carquin[34b], G.D. Carrillo-Montoya[32], J.R. Carter[30],
J. Carvalho[127a,127c], D. Casadei[19], M.P. Casado[13,h], M. Casolino[13], D.W. Casper[163],
E. Castaneda-Miranda[146a], A. Castelli[108], V. Castillo Gimenez[167], N.F. Castro[127a,i],
A. Catinaccio[32], J.R. Catmore[120], A. Cattai[32], J. Caudron[85], V. Cavaliere[166], E. Cavallaro[13],
D. Cavalli[93a], M. Cavalli-Sforza[13], V. Cavasinni[125a,125b], F. Ceradini[135a,135b],
L. Cerda Alberich[167], B.C. Cerio[47], A.S. Cerqueira[26b], A. Cerri[150], L. Cerrito[78], F. Cerutti[16],
M. Cerv[32], A. Cervelli[18], S.A. Cetin[20d], A. Chafaq[136a], D. Chakraborty[109], S.K. Chan[59],
Y.L. Chan[62a], P. Chang[166], J.D. Chapman[30], D.G. Charlton[19], A. Chatterjee[51], C.C. Chau[159],
C.A. Chavez Barajas[150], S. Che[112], S. Cheatham[74], A. Chegwidden[92], S. Chekanov[6],
S.V. Chekulaev[160a], G.A. Chelkov[67,j], M.A. Chelstowska[91], C. Chen[66], H. Chen[27], K. Chen[149],
S. Chen[35c], S. Chen[156], X. Chen[35f], Y. Chen[69], H.C. Cheng[91], H.J Cheng[35a], Y. Cheng[33],
A. Cheplakov[67], E. Cheremushkina[131], R. Cherkaoui El Moursli[136e], V. Chernyatin[27,*], E. Cheu[7],
L. Chevalier[137], V. Chiarella[49], G. Chiarelli[125a,125b], G. Chiodini[75a], A.S. Chisholm[19],
A. Chitan[28b], M.V. Chizhov[67], K. Choi[63], A.R. Chomont[36], S. Chouridou[9], B.K.B. Chow[101],
V. Christodoulou[80], D. Chromek-Burckhart[32], J. Chudoba[128], A.J. Chuinard[89],
J.J. Chwastowski[41], L. Chytka[116], G. Ciapetti[133a,133b], A.K. Ciftci[4a], D. Cinca[55], V. Cindro[77],
I.A. Cioara[23], A. Ciocio[16], F. Cirotto[105a,105b], Z.H. Citron[172], M. Ciubancan[28b], A. Clark[51],
B.L. Clark[59], M.R. Clark[37], P.J. Clark[48], R.N. Clarke[16], C. Clement[147a,147b], Y. Coadou[87],
M. Cobal[164a,164c], A. Coccaro[51], J. Cochran[66], L. Coffey[25], L. Colasurdo[107], B. Cole[37], S. Cole[109],
A.P. Colijn[108], J. Collot[57], T. Colombo[32], G. Compostella[102], P. Conde Muiño[127a,127b],
E. Coniavitis[50], S.H. Connell[146b], I.A. Connelly[79], V. Consorti[50], S. Constantinescu[28b],
C. Conta[122a,122b], G. Conti[32], F. Conventi[105a,k], M. Cooke[16], B.D. Cooper[80],
A.M. Cooper-Sarkar[121], T. Cornelissen[175], M. Corradi[133a,133b], F. Corriveau[89,l],
A. Corso-Radu[163], A. Cortes-Gonzalez[13], G. Cortiana[102], G. Costa[93a], M.J. Costa[167],
D. Costanzo[140], G. Cottin[30], G. Cowan[79], B.E. Cox[86], K. Cranmer[111], S.J. Crawley[55], G. Cree[31],
S. Crépé-Renaudin[57], F. Crescioli[82], W.A. Cribbs[147a,147b], M. Crispin Ortuzar[121],
M. Cristinziani[23], V. Croft[107], G. Crosetti[39a,39b], T. Cuhadar Donszelmann[140], J. Cummings[176],
M. Curatolo[49], J. Cúth[85], C. Cuthbert[151], H. Czirr[142], P. Czodrowski[3], S. D'Auria[55],
M. D'Onofrio[76], M.J. Da Cunha Sargedas De Sousa[127a,127b], C. Da Via[86], W. Dabrowski[40a],
T. Dai[91], O. Dale[15], F. Dallaire[96], C. Dallapiccola[88], M. Dam[38], J.R. Dandoy[33], N.P. Dang[50],
A.C. Daniells[19], N.S. Dann[86], M. Danninger[168], M. Dano Hoffmann[137], V. Dao[50], G. Darbo[52a],

S. Darmora[8], J. Dassoulas[3], A. Dattagupta[63], W. Davey[23], C. David[169], T. Davidek[130],
M. Davies[154], P. Davison[80], Y. Davygora[60a], E. Dawe[90], I. Dawson[140],
R.K. Daya-Ishmukhametova[88], K. De[8], R. de Asmundis[105a], A. De Benedetti[114],
S. De Castro[22a,22b], S. De Cecco[82], N. De Groot[107], P. de Jong[108], H. De la Torre[84],
F. De Lorenzi[66], D. De Pedis[133a], A. De Salvo[133a], U. De Sanctis[150], A. De Santo[150],
J.B. De Vivie De Regie[118], W.J. Dearnaley[74], R. Debbe[27], C. Debenedetti[138], D.V. Dedovich[67],
I. Deigaard[108], J. Del Peso[84], T. Del Prete[125a,125b], D. Delgove[118], F. Deliot[137], C.M. Delitzsch[51],
M. Deliyergiyev[77], A. Dell'Acqua[32], L. Dell'Asta[24], M. Dell'Orso[125a,125b], M. Della Pietra[105a,k],
D. della Volpe[51], M. Delmastro[5], P.A. Delsart[57], C. Deluca[108], D.A. DeMarco[159], S. Demers[176],
M. Demichev[67], A. Demilly[82], S.P. Denisov[131], D. Denysiuk[137], D. Derendarz[41],
J.E. Derkaoui[136d], F. Derue[82], P. Dervan[76], K. Desch[23], C. Deterre[44], K. Dette[45],
P.O. Deviveiros[32], A. Dewhurst[132], S. Dhaliwal[25], A. Di Ciaccio[134a,134b], L. Di Ciaccio[5],
W.K. Di Clemente[123], C. Di Donato[133a,133b], A. Di Girolamo[32], B. Di Girolamo[32],
B. Di Micco[135a,135b], R. Di Nardo[49], A. Di Simone[50], R. Di Sipio[159], D. Di Valentino[31],
C. Diaconu[87], M. Diamond[159], F.A. Dias[48], M.A. Diaz[34a], E.B. Diehl[91], J. Dietrich[17], S. Diglio[87],
A. Dimitrievska[14], J. Dingfelder[23], P. Dita[28b], S. Dita[28b], F. Dittus[32], F. Djama[87], T. Djobava[53b],
J.I. Djuvsland[60a], M.A.B. do Vale[26c], D. Dobos[32], M. Dobre[28b], C. Doglioni[83], T. Dohmae[156],
J. Dolejsi[130], Z. Dolezal[130], B.A. Dolgoshein[99,*], M. Donadelli[26d], S. Donati[125a,125b],
P. Dondero[122a,122b], J. Donini[36], J. Dopke[132], A. Doria[105a], M.T. Dova[73], A.T. Doyle[55],
E. Drechsler[56], M. Dris[10], Y. Du[35d], J. Duarte-Campderros[154], E. Duchovni[172], G. Duckeck[101],
O.A. Ducu[28b], D. Duda[108], A. Dudarev[32], L. Duflot[118], L. Duguid[79], M. Dührssen[32],
M. Dunford[60a], H. Duran Yildiz[4a], M. Düren[54], A. Durglishvili[53b], D. Duschinger[46], B. Dutta[44],
M. Dyndal[40a], C. Eckardt[44], K.M. Ecker[102], R.C. Edgar[91], W. Edson[2], N.C. Edwards[48],
T. Eifert[32], G. Eigen[15], K. Einsweiler[16], T. Ekelof[165], M. El Kacimi[136c], V. Ellajosyula[87],
M. Ellert[165], S. Elles[5], F. Ellinghaus[175], A.A. Elliot[169], N. Ellis[32], J. Elmsheuser[27], M. Elsing[32],
D. Emeliyanov[132], Y. Enari[156], O.C. Endner[85], M. Endo[119], J.S. Ennis[170], J. Erdmann[45],
A. Ereditato[18], G. Ernis[175], J. Ernst[2], M. Ernst[27], S. Errede[166], E. Ertel[85], M. Escalier[118],
H. Esch[45], C. Escobar[126], B. Esposito[49], A.I. Etienvre[137], E. Etzion[154], H. Evans[63], A. Ezhilov[124],
F. Fabbri[22a,22b], L. Fabbri[22a,22b], G. Facini[33], R.M. Fakhrutdinov[131], S. Falciano[133a], R.J. Falla[80],
J. Faltova[130], Y. Fang[35a], M. Fanti[93a,93b], A. Farbin[8], A. Farilla[135a], C. Farina[126], T. Farooque[13],
S. Farrell[16], S.M. Farrington[170], P. Farthouat[32], F. Fassi[136e], P. Fassnacht[32], D. Fassouliotis[9],
M. Faucci Giannelli[79], A. Favareto[52a,52b], W.J. Fawcett[121], L. Fayard[118], O.L. Fedin[124,m],
W. Fedorko[168], S. Feigl[120], L. Feligioni[87], C. Feng[35d], E.J. Feng[32], H. Feng[91], A.B. Fenyuk[131],
L. Feremenga[8], P. Fernandez Martinez[167], S. Fernandez Perez[13], J. Ferrando[55], A. Ferrari[165],
P. Ferrari[108], R. Ferrari[122a], D.E. Ferreira de Lima[55], A. Ferrer[167], D. Ferrere[51], C. Ferretti[91],
A. Ferretto Parodi[52a,52b], F. Fiedler[85], A. Filipčič[77], M. Filipuzzi[44], F. Filthaut[107],
M. Fincke-Keeler[169], K.D. Finelli[151], M.C.N. Fiolhais[127a,127c], L. Fiorini[167], A. Firan[42],
A. Fischer[2], C. Fischer[13], J. Fischer[175], W.C. Fisher[92], N. Flaschel[44], I. Fleck[142],
P. Fleischmann[91], G.T. Fletcher[140], G. Fletcher[78], R.R.M. Fletcher[123], T. Flick[175], A. Floderus[83],
L.R. Flores Castillo[62a], M.J. Flowerdew[102], G.T. Forcolin[86], A. Formica[137], A. Forti[86],
A.G. Foster[19], D. Fournier[118], H. Fox[74], S. Fracchia[13], P. Francavilla[82], M. Franchini[22a,22b],
D. Francis[32], L. Franconi[120], M. Franklin[59], M. Frate[163], M. Fraternali[122a,122b], D. Freeborn[80],
S.M. Fressard-Batraneanu[32], F. Friedrich[46], D. Froidevaux[32], J.A. Frost[121], C. Fukunaga[157],
E. Fullana Torregrosa[85], T. Fusayasu[103], J. Fuster[167], C. Gabaldon[57], O. Gabizon[175],
A. Gabrielli[22a,22b], A. Gabrielli[16], G.P. Gach[40a], S. Gadatsch[32], S. Gadomski[51],
G. Gagliardi[52a,52b], L.G. Gagnon[96], P. Gagnon[63], C. Galea[107], B. Galhardo[127a,127c],
E.J. Gallas[121], B.J. Gallop[132], P. Gallus[129], G. Galster[38], K.K. Gan[112], J. Gao[35b,87], Y. Gao[48],
Y.S. Gao[144,f], F.M. Garay Walls[48], C. García[167], J.E. García Navarro[167], M. Garcia-Sciveres[16],
R.W. Gardner[33], N. Garelli[144], V. Garonne[120], A. Gascon Bravo[44], C. Gatti[49],
A. Gaudiello[52a,52b], G. Gaudio[122a], B. Gaur[142], L. Gauthier[96], I.L. Gavrilenko[97], C. Gay[168],
G. Gaycken[23], E.N. Gazis[10], Z. Gecse[168], C.N.P. Gee[132], Ch. Geich-Gimbel[23], M.P. Geisler[60a],
C. Gemme[52a], M.H. Genest[57], C. Geng[35b,n], S. Gentile[133a,133b], S. George[79], D. Gerbaudo[163],

A. Gershon[154], S. Ghasemi[142], H. Ghazlane[136b], M. Ghneimat[23], B. Giacobbe[22a],
S. Giagu[133a,133b], P. Giannetti[125a,125b], B. Gibbard[27], S.M. Gibson[79], M. Gignac[168],
M. Gilchriese[16], T.P.S. Gillam[30], D. Gillberg[31], G. Gilles[175], D.M. Gingrich[3,d], N. Giokaris[9],
M.P. Giordani[164a,164c], F.M. Giorgi[22a], F.M. Giorgi[17], P.F. Giraud[137], P. Giromini[59],
D. Giugni[93a], F. Giuli[121], C. Giuliani[102], M. Giulini[60b], B.K. Gjelsten[120], S. Gkaitatzis[155],
I. Gkialas[155], E.L. Gkougkousis[118], L.K. Gladilin[100], C. Glasman[84], J. Glatzer[32],
P.C.F. Glaysher[48], A. Glazov[44], M. Goblirsch-Kolb[102], J. Godlewski[41], S. Goldfarb[91],
T. Golling[51], D. Golubkov[131], A. Gomes[127a,127b,127d], R. Gonçalo[127a],
J. Goncalves Pinto Firmino Da Costa[137], L. Gonella[19], A. Gongadze[67], S. González de la Hoz[167],
G. Gonzalez Parra[13], S. Gonzalez-Sevilla[51], L. Goossens[32], P.A. Gorbounov[98], H.A. Gordon[27],
I. Gorelov[106], B. Gorini[32], E. Gorini[75a,75b], A. Gorišek[77], E. Gornicki[41], A.T. Goshaw[47],
C. Gössling[45], M.I. Gostkin[67], C.R. Goudet[118], D. Goujdami[136c], A.G. Goussiou[139],
N. Govender[146b,o], E. Gozani[153], L. Graber[56], I. Grabowska-Bold[40a], P.O.J. Gradin[57],
P. Grafström[22a,22b], J. Gramling[51], E. Gramstad[120], S. Grancagnolo[17], V. Gratchev[124],
H.M. Gray[32], E. Graziani[135a], Z.D. Greenwood[81,p], C. Grefe[23], K. Gregersen[80], I.M. Gregor[44],
P. Grenier[144], K. Grevtsov[5], J. Griffiths[8], A.A. Grillo[138], K. Grimm[74], S. Grinstein[13,q],
Ph. Gris[36], J.-F. Grivaz[118], S. Groh[85], J.P. Grohs[46], E. Gross[172], J. Grosse-Knetter[56],
G.C. Grossi[81], Z.J. Grout[150], L. Guan[91], W. Guan[173], J. Guenther[129], F. Guescini[51], D. Guest[163],
O. Gueta[154], E. Guido[52a,52b], T. Guillemin[5], S. Guindon[2], U. Gul[55], C. Gumpert[32], J. Guo[35e],
Y. Guo[35b,n], S. Gupta[121], G. Gustavino[133a,133b], P. Gutierrez[114], N.G. Gutierrez Ortiz[80],
C. Gutschow[46], C. Guyot[137], C. Gwenlan[121], C.B. Gwilliam[76], A. Haas[111], C. Haber[16],
H.K. Hadavand[8], N. Haddad[136e], A. Hadef[87], P. Haefner[23], S. Hageböck[23], Z. Hajduk[41],
H. Hakobyan[177,*], M. Haleem[44], J. Haley[115], D. Hall[121], G. Halladjian[92], G.D. Hallewell[87],
K. Hamacher[175], P. Hamal[116], K. Hamano[169], A. Hamilton[146a], G.N. Hamity[140], P.G. Hamnett[44],
L. Han[35b], K. Hanagaki[68,r], K. Hanawa[156], M. Hance[138], B. Haney[123], P. Hanke[60a], R. Hanna[137],
J.B. Hansen[38], J.D. Hansen[38], M.C. Hansen[23], P.H. Hansen[38], K. Hara[161], A.S. Hard[173],
T. Harenberg[175], F. Hariri[118], S. Harkusha[94], R.D. Harrington[48], P.F. Harrison[170], F. Hartjes[108],
M. Hasegawa[69], Y. Hasegawa[141], A. Hasib[114], S. Hassani[137], S. Haug[18], R. Hauser[92],
L. Hauswald[46], M. Havranek[128], C.M. Hawkes[19], R.J. Hawkings[32], A.D. Hawkins[83], D. Hayden[92],
C.P. Hays[121], J.M. Hays[78], H.S. Hayward[76], S.J. Haywood[132], S.J. Head[19], T. Heck[85],
V. Hedberg[83], L. Heelan[8], S. Heim[123], T. Heim[16], B. Heinemann[16], J.J. Heinrich[101],
L. Heinrich[111], C. Heinz[54], J. Hejbal[128], L. Helary[24], S. Hellman[147a,147b], C. Helsens[32],
J. Henderson[121], R.C.W. Henderson[74], Y. Heng[173], S. Henkelmann[168], A.M. Henriques Correia[32],
S. Henrot-Versille[118], G.H. Herbert[17], Y. Hernández Jiménez[167], G. Herten[50], R. Hertenberger[101],
L. Hervas[32], G.G. Hesketh[80], N.P. Hessey[108], J.W. Hetherly[42], R. Hickling[78],
E. Higón-Rodriguez[167], E. Hill[169], J.C. Hill[30], K.H. Hiller[44], S.J. Hillier[19], I. Hinchliffe[16],
E. Hines[123], R.R. Hinman[16], M. Hirose[158], D. Hirschbuehl[175], J. Hobbs[149], N. Hod[108],
M.C. Hodgkinson[140], P. Hodgson[140], A. Hoecker[32], M.R. Hoeferkamp[106], F. Hoenig[101],
M. Hohlfeld[85], D. Hohn[23], T.R. Holmes[16], M. Homann[45], T.M. Hong[126], B.H. Hooberman[166],
W.H. Hopkins[117], Y. Horii[104], A.J. Horton[143], J-Y. Hostachy[57], S. Hou[152], A. Hoummada[136a],
J. Howard[121], J. Howarth[44], M. Hrabovsky[116], I. Hristova[17], J. Hrivnac[118], T. Hryn'ova[5],
A. Hrynevich[95], C. Hsu[146c], P.J. Hsu[152,s], S.-C. Hsu[139], D. Hu[37], Q. Hu[35b], Y. Huang[44],
Z. Hubacek[129], F. Hubaut[87], F. Huegging[23], T.B. Huffman[121], E.W. Hughes[37], G. Hughes[74],
M. Huhtinen[32], T.A. Hülsing[85], P. Huo[149], N. Huseynov[67,b], J. Huston[92], J. Huth[59],
G. Iacobucci[51], G. Iakovidis[27], I. Ibragimov[142], L. Iconomidou-Fayard[118], E. Ideal[176],
Z. Idrissi[136e], P. Iengo[32], O. Igonkina[108,t], T. Iizawa[171], Y. Ikegami[68], M. Ikeno[68], Y. Ilchenko[11,u],
D. Iliadis[155], N. Ilic[144], T. Ince[102], G. Introzzi[122a,122b], P. Ioannou[9,*], M. Iodice[135a],
K. Iordanidou[37], V. Ippolito[59], A. Irles Quiles[167], C. Isaksson[165], M. Ishino[70], M. Ishitsuka[158],
R. Ishmukhametov[112], C. Issever[121], S. Istin[20a], F. Ito[161], J.M. Iturbe Ponce[86], R. Iuppa[134a,134b],
J. Ivarsson[83], W. Iwanski[41], H. Iwasaki[68], J.M. Izen[43], V. Izzo[105a], S. Jabbar[3], B. Jackson[123],
M. Jackson[76], P. Jackson[1], V. Jain[2], K.B. Jakobi[85], K. Jakobs[50], S. Jakobsen[32], T. Jakoubek[128],
D.O. Jamin[115], D.K. Jana[81], E. Jansen[80], R. Jansky[64], J. Janssen[23], M. Janus[56], G. Jarlskog[83],

N. Javadov[67,b], T. Javůrek[50], F. Jeanneau[137], L. Jeanty[16], J. Jejelava[53a,v], G.-Y. Jeng[151],
D. Jennens[90], P. Jenni[50,w], J. Jentzsch[45], C. Jeske[170], S. Jézéquel[5], H. Ji[173], J. Jia[149], H. Jiang[66],
Y. Jiang[35b], S. Jiggins[80], J. Jimenez Pena[167], S. Jin[35a], A. Jinaru[28b], O. Jinnouchi[158],
P. Johansson[140], K.A. Johns[7], W.J. Johnson[139], K. Jon-And[147a,147b], G. Jones[170], R.W.L. Jones[74],
S. Jones[7], T.J. Jones[76], J. Jongmanns[60a], P.M. Jorge[127a,127b], J. Jovicevic[160a], X. Ju[173],
A. Juste Rozas[13,q], M.K. Köhler[172], A. Kaczmarska[41], M. Kado[118], H. Kagan[112], M. Kagan[144],
S.J. Kahn[87], E. Kajomovitz[47], C.W. Kalderon[121], A. Kaluza[85], S. Kama[42], A. Kamenshchikov[131],
N. Kanaya[156], S. Kaneti[30], L. Kanjir[77], V.A. Kantserov[99], J. Kanzaki[68], B. Kaplan[111],
L.S. Kaplan[173], A. Kapliy[33], D. Kar[146c], K. Karakostas[10], A. Karamaoun[3], N. Karastathis[10],
M.J. Kareem[56], E. Karentzos[10], M. Karnevskiy[85], S.N. Karpov[67], Z.M. Karpova[67], K. Karthik[111],
V. Kartvelishvili[74], A.N. Karyukhin[131], K. Kasahara[161], L. Kashif[173], R.D. Kass[112],
A. Kastanas[15], Y. Kataoka[156], C. Kato[156], A. Katre[51], J. Katzy[44], K. Kawagoe[72],
T. Kawamoto[156], G. Kawamura[56], S. Kazama[156], V.F. Kazanin[110,c], R. Keeler[169], R. Kehoe[42],
J.S. Keller[44], J.J. Kempster[79], K Kentaro[104], H. Keoshkerian[86], O. Kepka[128], B.P. Kerševan[77],
S. Kersten[175], R.A. Keyes[89], F. Khalil-zada[12], H. Khandanyan[147a,147b], A. Khanov[115],
A.G. Kharlamov[110,c], T.J. Khoo[30], V. Khovanskiy[98], E. Khramov[67], J. Khubua[53b,x], S. Kido[69],
H.Y. Kim[8], S.H. Kim[161], Y.K. Kim[33], N. Kimura[155], O.M. Kind[17], B.T. King[76], M. King[167],
S.B. King[168], J. Kirk[132], A.E. Kiryunin[102], T. Kishimoto[69], D. Kisielewska[40a], F. Kiss[50],
K. Kiuchi[161], O. Kivernyk[137], E. Kladiva[145b], M.H. Klein[37], M. Klein[76], U. Klein[76],
K. Kleinknecht[85], P. Klimek[147a,147b], A. Klimentov[27], R. Klingenberg[45], J.A. Klinger[140],
T. Klioutchnikova[32], E.-E. Kluge[60a], P. Kluit[108], S. Kluth[102], J. Knapik[41], E. Kneringer[64],
E.B.F.G. Knoops[87], A. Knue[55], A. Kobayashi[156], D. Kobayashi[158], T. Kobayashi[156], M. Kobel[46],
M. Kocian[144], P. Kodys[130], T. Koffas[31], E. Koffeman[108], L.A. Kogan[121], T. Koi[144],
H. Kolanoski[17], M. Kolb[60b], I. Koletsou[5], A.A. Komar[97,*], Y. Komori[156], T. Kondo[68],
N. Kondrashova[44], K. Köneke[50], A.C. König[107], T. Kono[68,y], R. Konoplich[111,z],
N. Konstantinidis[80], R. Kopeliansky[63], S. Koperny[40a], L. Köpke[85], A.K. Kopp[50], K. Korcyl[41],
K. Kordas[155], A. Korn[80], A.A. Korol[110,c], I. Korolkov[13], E.V. Korolkova[140], O. Kortner[102],
S. Kortner[102], T. Kosek[130], V.V. Kostyukhin[23], A. Kotwal[47], A. Kourkoumeli-Charalampidi[155],
C. Kourkoumelis[9], V. Kouskoura[27], A. Koutsman[160a], A.B. Kowalewska[41], R. Kowalewski[169],
T.Z. Kowalski[40a], W. Kozanecki[137], A.S. Kozhin[131], V.A. Kramarenko[100], G. Kramberger[77],
D. Krasnopevtsev[99], M.W. Krasny[82], A. Krasznahorkay[32], J.K. Kraus[23], A. Kravchenko[27],
M. Kretz[60c], J. Kretzschmar[76], K. Kreutzfeldt[54], P. Krieger[159], K. Krizka[33], K. Kroeninger[45],
H. Kroha[102], J. Kroll[123], J. Kroseberg[23], J. Krstic[14], U. Kruchonak[67], H. Krüger[23],
N. Krumnack[66], A. Kruse[173], M.C. Kruse[47], M. Kruskal[24], T. Kubota[90], H. Kucuk[80], S. Kuday[4b],
J.T. Kuechler[175], S. Kuehn[50], A. Kugel[60c], F. Kuger[174], A. Kuhl[138], T. Kuhl[44], V. Kukhtin[67],
R. Kukla[137], Y. Kulchitsky[94], S. Kuleshov[34b], M. Kuna[133a,133b], T. Kunigo[70], A. Kupco[128],
H. Kurashige[69], Y.A. Kurochkin[94], V. Kus[128], E.S. Kuwertz[169], M. Kuze[158], J. Kvita[116],
T. Kwan[169], D. Kyriazopoulos[140], A. La Rosa[102], J.L. La Rosa Navarro[26d], L. La Rotonda[39a,39b],
C. Lacasta[167], F. Lacava[133a,133b], J. Lacey[31], H. Lacker[17], D. Lacour[82], V.R. Lacuesta[167],
E. Ladygin[67], R. Lafaye[5], B. Laforge[82], T. Lagouri[176], S. Lai[56], S. Lammers[63], W. Lampl[7],
E. Lançon[137], U. Landgraf[50], M.P.J. Landon[78], V.S. Lang[60a], J.C. Lange[13], A.J. Lankford[163],
F. Lanni[27], K. Lantzsch[23], A. Lanza[122a], S. Laplace[82], C. Lapoire[32], J.F. Laporte[137], T. Lari[93a],
F. Lasagni Manghi[22a,22b], M. Lassnig[32], P. Laurelli[49], W. Lavrijsen[16], A.T. Law[138], P. Laycock[76],
T. Lazovich[59], M. Lazzaroni[93a,93b], O. Le Dortz[82], E. Le Guirriec[87], E. Le Menedeu[13],
E.P. Le Quilleuc[137], M. LeBlanc[169], T. LeCompte[6], F. Ledroit-Guillon[57], C.A. Lee[27], S.C. Lee[152],
L. Lee[1], G. Lefebvre[82], M. Lefebvre[169], F. Legger[101], C. Leggett[16], A. Lehan[76],
G. Lehmann Miotto[32], X. Lei[7], W.A. Leight[31], A. Leisos[155,aa], A.G. Leister[176], M.A.L. Leite[26d],
R. Leitner[130], D. Lellouch[172], B. Lemmer[56], K.J.C. Leney[80], T. Lenz[23], B. Lenzi[32], R. Leone[7],
S. Leone[125a,125b], C. Leonidopoulos[48], S. Leontsinis[10], G. Lerner[150], C. Leroy[96], A.A.J. Lesage[137],
C.G. Lester[30], M. Levchenko[124], J. Levêque[5], D. Levin[91], L.J. Levinson[172], M. Levy[19],
A.M. Leyko[23], M. Leyton[43], B. Li[35b,n], H. Li[149], H.L. Li[33], L. Li[47], L. Li[35e], Q. Li[35a], S. Li[47],
X. Li[86], Y. Li[142], Z. Liang[138], H. Liao[36], B. Liberti[134a], A. Liblong[159], P. Lichard[32], K. Lie[166],

J. Liebal[23], W. Liebig[15], C. Limbach[23], A. Limosani[151], S.C. Lin[152,ab], T.H. Lin[85],
B.E. Lindquist[149], E. Lipeles[123], A. Lipniacka[15], M. Lisovyi[60b], T.M. Liss[166], D. Lissauer[27],
A. Lister[168], A.M. Litke[138], B. Liu[152,ac], D. Liu[152], H. Liu[91], H. Liu[27], J. Liu[87], J.B. Liu[35b],
K. Liu[87], L. Liu[166], M. Liu[47], M. Liu[35b], Y.L. Liu[35b], Y. Liu[35b], M. Livan[122a,122b], A. Lleres[57],
J. Llorente Merino[84], S.L. Lloyd[78], F. Lo Sterzo[152], E. Lobodzinska[44], P. Loch[7],
W.S. Lockman[138], F.K. Loebinger[86], A.E. Loevschall-Jensen[38], K.M. Loew[25], A. Loginov[176],
T. Lohse[17], K. Lohwasser[44], M. Lokajicek[128], B.A. Long[24], J.D. Long[166], R.E. Long[74],
L. Longo[75a,75b], K.A. Looper[112], L. Lopes[127a], D. Lopez Mateos[59], B. Lopez Paredes[140],
I. Lopez Paz[13], A. Lopez Solis[82], J. Lorenz[101], N. Lorenzo Martinez[63], M. Losada[21], P.J. Lösel[101],
X. Lou[35a], A. Lounis[118], J. Love[6], P.A. Love[74], H. Lu[62a], N. Lu[91], H.J. Lubatti[139],
C. Luci[133a,133b], A. Lucotte[57], C. Luedtke[50], F. Luehring[63], W. Lukas[64], L. Luminari[133a],
O. Lundberg[147a,147b], B. Lund-Jensen[148], D. Lynn[27], R. Lysak[128], E. Lytken[83], V. Lyubushkin[67],
H. Ma[27], L.L. Ma[35d], Y. Ma[35d], G. Maccarrone[49], A. Macchiolo[102], C.M. Macdonald[140],
B. Maček[77], J. Machado Miguens[123,127b], D. Madaffari[87], R. Madar[36], H.J. Maddocks[165],
W.F. Mader[46], A. Madsen[44], J. Maeda[69], S. Maeland[15], T. Maeno[27], A. Maevskiy[100],
E. Magradze[56], J. Mahlstedt[108], C. Maiani[118], C. Maidantchik[26a], A.A. Maier[102], T. Maier[101],
A. Maio[127a,127b,127d], S. Majewski[117], Y. Makida[68], N. Makovec[118], B. Malaescu[82], Pa. Malecki[41],
V.P. Maleev[124], F. Malek[57], U. Mallik[65], D. Malon[6], C. Malone[144], S. Maltezos[10], S. Malyukov[32],
J. Mamuzic[167], G. Mancini[49], B. Mandelli[32], L. Mandelli[93a], I. Mandić[77], J. Maneira[127a,127b],
L. Manhaes de Andrade Filho[26b], J. Manjarres Ramos[160b], A. Mann[101], B. Mansoulie[137],
R. Mantifel[89], M. Mantoani[56], S. Manzoni[93a,93b], L. Mapelli[32], G. Marceca[29], L. March[51],
G. Marchiori[82], M. Marcisovsky[128], M. Marjanovic[14], D.E. Marley[91], F. Marroquim[26a],
S.P. Marsden[86], Z. Marshall[16], L.F. Marti[18], S. Marti-Garcia[167], B. Martin[92], T.A. Martin[170],
V.J. Martin[48], B. Martin dit Latour[15], M. Martinez[13,q], S. Martin-Haugh[132], V.S. Martoiu[28b],
A.C. Martyniuk[80], M. Marx[139], F. Marzano[133a], A. Marzin[32], L. Masetti[85], T. Mashimo[156],
R. Mashinistov[97], J. Masik[86], A.L. Maslennikov[110,c], I. Massa[22a,22b], L. Massa[22a,22b],
P. Mastrandrea[5], A. Mastroberardino[39a,39b], T. Masubuchi[156], P. Mättig[175], J. Mattmann[85],
J. Maurer[28b], S.J. Maxfield[76], D.A. Maximov[110,c], R. Mazini[152], S.M. Mazza[93a,93b],
N.C. Mc Fadden[106], G. Mc Goldrick[159], S.P. Mc Kee[91], A. McCarn[91], R.L. McCarthy[149],
T.G. McCarthy[31], L.I. McClymont[80], K.W. McFarlane[58,*], J.A. Mcfayden[80], G. Mchedlidze[56],
S.J. McMahon[132], R.A. McPherson[169,l], M. Medinnis[44], S. Meehan[139], S. Mehlhase[101],
A. Mehta[76], K. Meier[60a], C. Meineck[101], B. Meirose[43], B.R. Mellado Garcia[146c], F. Meloni[18],
A. Mengarelli[22a,22b], S. Menke[102], E. Meoni[162], K.M. Mercurio[59], S. Mergelmeyer[17], P. Mermod[51],
L. Merola[105a,105b], C. Meroni[93a], F.S. Merritt[33], A. Messina[133a,133b], J. Metcalfe[6], A.S. Mete[163],
C. Meyer[85], C. Meyer[123], J-P. Meyer[137], J. Meyer[108], H. Meyer Zu Theenhausen[60a],
R.P. Middleton[132], S. Miglioranzi[164a,164c], L. Mijović[23], G. Mikenberg[172], M. Mikestikova[128],
M. Mikuž[77], M. Milesi[90], A. Milic[32], D.W. Miller[33], C. Mills[48], A. Milov[172],
D.A. Milstead[147a,147b], A.A. Minaenko[131], Y. Minami[156], I.A. Minashvili[67], A.I. Mincer[111],
B. Mindur[40a], M. Mineev[67], Y. Ming[173], L.M. Mir[13], K.P. Mistry[123], T. Mitani[171],
J. Mitrevski[101], V.A. Mitsou[167], A. Miucci[51], P.S. Miyagawa[140], J.U. Mjörnmark[83],
T. Moa[147a,147b], K. Mochizuki[87], S. Mohapatra[37], W. Mohr[50], S. Molander[147a,147b],
R. Moles-Valls[23], R. Monden[70], M.C. Mondragon[92], K. Mönig[44], J. Monk[38], E. Monnier[87],
A. Montalbano[149], J. Montejo Berlingen[32], F. Monticelli[73], S. Monzani[93a,93b], R.W. Moore[3],
N. Morange[118], D. Moreno[21], M. Moreno Llácer[56], P. Morettini[52a], D. Mori[143], T. Mori[156],
M. Morii[59], M. Morinaga[156], V. Morisbak[120], S. Moritz[85], A.K. Morley[151], G. Mornacchi[32],
J.D. Morris[78], S.S. Mortensen[38], L. Morvaj[149], M. Mosidze[53b], J. Moss[144], K. Motohashi[158],
R. Mount[144], E. Mountricha[27], S.V. Mouraviev[97,*], E.J.W. Moyse[88], S. Muanza[87], R.D. Mudd[19],
F. Mueller[102], J. Mueller[126], R.S.P. Mueller[101], T. Mueller[30], D. Muenstermann[74], P. Mullen[55],
G.A. Mullier[18], F.J. Munoz Sanchez[86], J.A. Murillo Quijada[19], W.J. Murray[170,132],
H. Musheghyan[56], M. Muškinja[77], A.G. Myagkov[131,ad], M. Myska[129], B.P. Nachman[144],
O. Nackenhorst[51], J. Nadal[56], K. Nagai[121], R. Nagai[68,y], K. Nagano[68], Y. Nagasaka[61],
K. Nagata[161], M. Nagel[102], E. Nagy[87], A.M. Nairz[32], Y. Nakahama[32], K. Nakamura[68],

T. Nakamura[156], I. Nakano[113], H. Namasivayam[43], R.F. Naranjo Garcia[44], R. Narayan[11],
D.I. Narrias Villar[60a], I. Naryshkin[124], T. Naumann[44], G. Navarro[21], R. Nayyar[7], H.A. Neal[91],
P.Yu. Nechaeva[97], T.J. Neep[86], P.D. Nef[144], A. Negri[122a,122b], M. Negrini[22a], S. Nektarijevic[107],
C. Nellist[118], A. Nelson[163], S. Nemecek[128], P. Nemethy[111], A.A. Nepomuceno[26a], M. Nessi[32,ae],
M.S. Neubauer[166], M. Neumann[175], R.M. Neves[111], P. Nevski[27], P.R. Newman[19], D.H. Nguyen[6],
R.B. Nickerson[121], R. Nicolaidou[137], B. Nicquevert[32], J. Nielsen[138], A. Nikiforov[17],
V. Nikolaenko[131,ad], I. Nikolic-Audit[82], K. Nikolopoulos[19], J.K. Nilsen[120], P. Nilsson[27],
Y. Ninomiya[156], A. Nisati[133a], R. Nisius[102], T. Nobe[156], L. Nodulman[6], M. Nomachi[119],
I. Nomidis[31], T. Nooney[78], S. Norberg[114], M. Nordberg[32], N. Norjoharuddeen[121],
O. Novgorodova[46], S. Nowak[102], M. Nozaki[68], L. Nozka[116], K. Ntekas[10], E. Nurse[80], F. Nuti[90],
F. O'grady[7], D.C. O'Neil[143], A.A. O'Rourke[44], V. O'Shea[55], F.G. Oakham[31,d], H. Oberlack[102],
T. Obermann[23], J. Ocariz[82], A. Ochi[69], I. Ochoa[37], J.P. Ochoa-Ricoux[34a], S. Oda[72], S. Odaka[68],
H. Ogren[63], A. Oh[86], S.H. Oh[47], C.C. Ohm[16], H. Ohman[165], H. Oide[32], H. Okawa[161],
Y. Okumura[33], T. Okuyama[68], A. Olariu[28b], L.F. Oleiro Seabra[127a], S.A. Olivares Pino[48],
D. Oliveira Damazio[27], A. Olszewski[41], J. Olszowska[41], A. Onofre[127a,127e], K. Onogi[104],
P.U.E. Onyisi[11,u], C.J. Oram[160a], M.J. Oreglia[33], Y. Oren[154], D. Orestano[135a,135b],
N. Orlando[62b], R.S. Orr[159], B. Osculati[52a,52b], R. Ospanov[86], G. Otero y Garzon[29], H. Otono[72],
M. Ouchrif[136d], F. Ould-Saada[120], A. Ouraou[137], K.P. Oussoren[108], Q. Ouyang[35a], M. Owen[55],
R.E. Owen[19], V.E. Ozcan[20a], N. Ozturk[8], K. Pachal[143], A. Pacheco Pages[13], C. Padilla Aranda[13],
M. Pagáčová[50], S. Pagan Griso[16], F. Paige[27], P. Pais[88], K. Pajchel[120], G. Palacino[160b],
S. Palestini[32], M. Palka[40b], D. Pallin[36], A. Palma[127a,127b], E.St. Panagiotopoulou[10],
C.E. Pandini[82], J.G. Panduro Vazquez[79], P. Pani[147a,147b], S. Panitkin[27], D. Pantea[28b],
L. Paolozzi[51], Th.D. Papadopoulou[10], K. Papageorgiou[155], A. Paramonov[6],
D. Paredes Hernandez[176], A.J. Parker[74], M.A. Parker[30], K.A. Parker[140], F. Parodi[52a,52b],
J.A. Parsons[37], U. Parzefall[50], V.R. Pascuzzi[159], E. Pasqualucci[133a], S. Passaggio[52a],
F. Pastore[135a,135b,*], Fr. Pastore[79], G. Pásztor[31,af], S. Pataraia[175], N.D. Patel[151], J.R. Pater[86],
T. Pauly[32], J. Pearce[169], B. Pearson[114], L.E. Pedersen[38], M. Pedersen[120], S. Pedraza Lopez[167],
R. Pedro[127a,127b], S.V. Peleganchuk[110,c], D. Pelikan[165], O. Penc[128], C. Peng[35a], H. Peng[35b],
J. Penwell[63], B.S. Peralva[26b], M.M. Perego[137], D.V. Perepelitsa[27], E. Perez Codina[160a],
L. Perini[93a,93b], H. Pernegger[32], S. Perrella[105a,105b], R. Peschke[44], V.D. Peshekhonov[67],
K. Peters[44], R.F.Y. Peters[86], B.A. Petersen[32], T.C. Petersen[38], E. Petit[57], A. Petridis[1],
C. Petridou[155], P. Petroff[118], E. Petrolo[133a], M. Petrov[121], F. Petrucci[135a,135b],
N.E. Pettersson[158], A. Peyaud[137], R. Pezoa[34b], P.W. Phillips[132], G. Piacquadio[144], E. Pianori[170],
A. Picazio[88], E. Piccaro[78], M. Piccinini[22a,22b], M.A. Pickering[121], R. Piegaia[29], J.E. Pilcher[33],
A.D. Pilkington[86], A.W.J. Pin[86], J. Pina[127a,127b,127d], M. Pinamonti[164a,164c,ag], J.L. Pinfold[3],
A. Pingel[38], S. Pires[82], H. Pirumov[44], M. Pitt[172], L. Plazak[145a], M.-A. Pleier[27], V. Pleskot[85],
E. Plotnikova[67], P. Plucinski[147a,147b], D. Pluth[66], R. Poettgen[147a,147b], L. Poggioli[118], D. Pohl[23],
G. Polesello[122a], A. Poley[44], A. Policicchio[39a,39b], R. Polifka[159], A. Polini[22a], C.S. Pollard[55],
V. Polychronakos[27], K. Pommès[32], L. Pontecorvo[133a], B.G. Pope[92], G.A. Popeneciu[28c],
D.S. Popovic[14], A. Poppleton[32], S. Pospisil[129], K. Potamianos[16], I.N. Potrap[67], C.J. Potter[30],
C.T. Potter[117], G. Poulard[32], J. Poveda[32], V. Pozdnyakov[67], M.E. Pozo Astigarraga[32],
P. Pralavorio[87], A. Pranko[16], S. Prell[66], D. Price[86], L.E. Price[6], M. Primavera[75a], S. Prince[89],
M. Proissl[48], K. Prokofiev[62c], F. Prokoshin[34b], S. Protopopescu[27], J. Proudfoot[6],
M. Przybycien[40a], D. Puddu[135a,135b], D. Puldon[149], M. Purohit[27,ah], P. Puzo[118], J. Qian[91],
G. Qin[55], Y. Qin[86], A. Quadt[56], W.B. Quayle[164a,164b], M. Queitsch-Maitland[86], D. Quilty[55],
S. Raddum[120], V. Radeka[27], V. Radescu[60b], S.K. Radhakrishnan[149], P. Radloff[117], P. Rados[90],
F. Ragusa[93a,93b], G. Rahal[178], J.A. Raine[86], S. Rajagopalan[27], M. Rammensee[32],
C. Rangel-Smith[165], M.G. Ratti[93a,93b], F. Rauscher[101], S. Rave[85], T. Ravenscroft[55],
M. Raymond[32], A.L. Read[120], N.P. Readioff[76], D.M. Rebuzzi[122a,122b], A. Redelbach[174],
G. Redlinger[27], R. Reece[138], K. Reeves[43], L. Rehnisch[17], J. Reichert[123], H. Reisin[29],
C. Rembser[32], H. Ren[35a], M. Rescigno[133a], S. Resconi[93a], O.L. Rezanova[110,c], P. Reznicek[130],
R. Rezvani[96], R. Richter[102], S. Richter[80], E. Richter-Was[40b], O. Ricken[23], M. Ridel[82], P. Rieck[17],

C.J. Riegel[175], J. Rieger[56], O. Rifki[114], M. Rijssenbeek[149], A. Rimoldi[122a,122b], L. Rinaldi[22a],
B. Ristić[51], E. Ritsch[32], I. Riu[13], F. Rizatdinova[115], E. Rizvi[78], C. Rizzi[13], S.H. Robertson[89,l],
A. Robichaud-Veronneau[89], D. Robinson[30], J.E.M. Robinson[44], A. Robson[55], C. Roda[125a,125b],
Y. Rodina[87], A. Rodriguez Perez[13], D. Rodriguez Rodriguez[167], S. Roe[32], C.S. Rogan[59],
O. Røhne[120], A. Romaniouk[99], M. Romano[22a,22b], S.M. Romano Saez[36], E. Romero Adam[167],
N. Rompotis[139], M. Ronzani[50], L. Roos[82], E. Ros[167], S. Rosati[133a], K. Rosbach[50], P. Rose[138],
O. Rosenthal[142], V. Rossetti[147a,147b], E. Rossi[105a,105b], L.P. Rossi[52a], J.H.N. Rosten[30],
R. Rosten[139], M. Rotaru[28b], I. Roth[172], J. Rothberg[139], D. Rousseau[118], C.R. Royon[137],
A. Rozanov[87], Y. Rozen[153], X. Ruan[146c], F. Rubbo[144], I. Rubinskiy[44], V.I. Rud[100],
M.S. Rudolph[159], F. Rühr[50], A. Ruiz-Martinez[32], Z. Rurikova[50], N.A. Rusakovich[67],
A. Ruschke[101], H.L. Russell[139], J.P. Rutherfoord[7], N. Ruthmann[32], Y.F. Ryabov[124], M. Rybar[166],
G. Rybkin[118], S. Ryu[6], A. Ryzhov[131], A.F. Saavedra[151], G. Sabato[108], S. Sacerdoti[29],
H.F-W. Sadrozinski[138], R. Sadykov[67], F. Safai Tehrani[133a], P. Saha[109], M. Sahinsoy[60a],
M. Saimpert[137], T. Saito[156], H. Sakamoto[156], Y. Sakurai[171], G. Salamanna[135a,135b],
A. Salamon[134a,134b], J.E. Salazar Loyola[34b], D. Salek[108], P.H. Sales De Bruin[139], D. Salihagic[102],
A. Salnikov[144], J. Salt[167], D. Salvatore[39a,39b], F. Salvatore[150], A. Salvucci[62a], A. Salzburger[32],
D. Sammel[50], D. Sampsonidis[155], A. Sanchez[105a,105b], J. Sánchez[167], V. Sanchez Martinez[167],
H. Sandaker[120], R.L. Sandbach[78], H.G. Sander[85], M.P. Sanders[101], M. Sandhoff[175], C. Sandoval[21],
R. Sandstroem[102], D.P.C. Sankey[132], M. Sannino[52a,52b], A. Sansoni[49], C. Santoni[36],
R. Santonico[134a,134b], H. Santos[127a], I. Santoyo Castillo[150], K. Sapp[126], A. Sapronov[67],
J.G. Saraiva[127a,127d], B. Sarrazin[23], O. Sasaki[68], Y. Sasaki[156], K. Sato[161], G. Sauvage[5,*],
E. Sauvan[5], G. Savage[79], P. Savard[159,d], C. Sawyer[132], L. Sawyer[81,p], J. Saxon[33], C. Sbarra[22a],
A. Sbrizzi[22a,22b], T. Scanlon[80], D.A. Scannicchio[163], M. Scarcella[151], V. Scarfone[39a,39b],
J. Schaarschmidt[172], P. Schacht[102], D. Schaefer[32], R. Schaefer[44], J. Schaeffer[85], S. Schaepe[23],
S. Schaetzel[60b], U. Schäfer[85], A.C. Schaffer[118], D. Schaile[101], R.D. Schamberger[149], V. Scharf[60a],
V.A. Schegelsky[124], D. Scheirich[130], M. Schernau[163], C. Schiavi[52a,52b], C. Schillo[50],
M. Schioppa[39a,39b], S. Schlenker[32], K. Schmieden[32], C. Schmitt[85], S. Schmitt[44], S. Schmitz[85],
B. Schneider[160a], Y.J. Schnellbach[76], U. Schnoor[50], L. Schoeffel[137], A. Schoening[60b],
B.D. Schoenrock[92], E. Schopf[23], A.L.S. Schorlemmer[45], M. Schott[85], J. Schovancova[8],
S. Schramm[51], M. Schreyer[174], N. Schuh[85], M.J. Schultens[23], H.-C. Schultz-Coulon[60a],
H. Schulz[17], M. Schumacher[50], B.A. Schumm[138], Ph. Schune[137], C. Schwanenberger[86],
A. Schwartzman[144], T.A. Schwarz[91], Ph. Schwegler[102], H. Schweiger[86], Ph. Schwemling[137],
R. Schwienhorst[92], J. Schwindling[137], T. Schwindt[23], G. Sciolla[25], F. Scuri[125a,125b], F. Scutti[90],
J. Searcy[91], P. Seema[23], S.C. Seidel[106], A. Seiden[138], F. Seifert[129], J.M. Seixas[26a],
G. Sekhniaidze[105a], K. Sekhon[91], S.J. Sekula[42], D.M. Seliverstov[124,*], N. Semprini-Cesari[22a,22b],
C. Serfon[120], L. Serin[118], L. Serkin[164a,164b], M. Sessa[135a,135b], R. Seuster[160a], H. Severini[114],
T. Sfiligoj[77], F. Sforza[32], A. Sfyrla[51], E. Shabalina[56], N.W. Shaikh[147a,147b], L.Y. Shan[35a],
R. Shang[166], J.T. Shank[24], M. Shapiro[16], P.B. Shatalov[98], K. Shaw[164a,164b], S.M. Shaw[86],
A. Shcherbakova[147a,147b], C.Y. Shehu[150], P. Sherwood[80], L. Shi[152,ai], S. Shimizu[69],
C.O. Shimmin[163], M. Shimojima[103], M. Shiyakova[67,aj], A. Shmeleva[97], D. Shoaleh Saadi[96],
M.J. Shochet[33], S. Shojaii[93a,93b], S. Shrestha[112], E. Shulga[99], M.A. Shupe[7], P. Sicho[128],
P.E. Sidebo[148], O. Sidiropoulou[174], D. Sidorov[115], A. Sidoti[22a,22b], F. Siegert[46], Dj. Sijacki[14],
J. Silva[127a,127d], S.B. Silverstein[147a], V. Simak[129], O. Simard[5], Lj. Simic[14], S. Simion[118],
E. Simioni[85], B. Simmons[80], D. Simon[36], M. Simon[85], P. Sinervo[159], N.B. Sinev[117],
M. Sioli[22a,22b], G. Siragusa[174], S.Yu. Sivoklokov[100], J. Sjölin[147a,147b], T.B. Sjursen[15],
M.B. Skinner[74], H.P. Skottowe[59], P. Skubic[114], M. Slater[19], T. Slavicek[129], M. Slawinska[108],
K. Sliwa[162], R. Slovak[130], V. Smakhtin[172], B.H. Smart[5], L. Smestad[15], S.Yu. Smirnov[99],
Y. Smirnov[99], L.N. Smirnova[100,ak], O. Smirnova[83], M.N.K. Smith[37], R.W. Smith[37],
M. Smizanska[74], K. Smolek[129], A.A. Snesarev[97], G. Snidero[78], S. Snyder[27], R. Sobie[169,l],
F. Socher[46], A. Soffer[154], D.A. Soh[152,ai], G. Sokhrannyi[77], C.A. Solans Sanchez[32], M. Solar[129],
E.Yu. Soldatov[99], U. Soldevila[167], A.A. Solodkov[131], A. Soloshenko[67], O.V. Solovyanov[131],
V. Solovyev[124], P. Sommer[50], H. Son[162], H.Y. Song[35b,al], A. Sood[16], A. Sopczak[129], V. Sopko[129],

V. Sorin[13], D. Sosa[60b], C.L. Sotiropoulou[125a,125b], R. Soualah[164a,164c], A.M. Soukharev[110,c],
D. South[44], B.C. Sowden[79], S. Spagnolo[75a,75b], M. Spalla[125a,125b], M. Spangenberg[170],
F. Spanò[79], D. Sperlich[17], F. Spettel[102], R. Spighi[22a], G. Spigo[32], L.A. Spiller[90], M. Spousta[130],
R.D. St. Denis[55,*], A. Stabile[93a], J. Stahlman[123], R. Stamen[60a], S. Stamm[17], E. Stanecka[41],
R.W. Stanek[6], C. Stanescu[135a], M. Stanescu-Bellu[44], M.M. Stanitzki[44], S. Stapnes[120],
E.A. Starchenko[131], G.H. Stark[33], J. Stark[57], P. Staroba[128], P. Starovoitov[60a], S. Stärz[32],
R. Staszewski[41], P. Steinberg[27], B. Stelzer[143], H.J. Stelzer[32], O. Stelzer-Chilton[160a], H. Stenzel[54],
G.A. Stewart[55], J.A. Stillings[23], M.C. Stockton[89], M. Stoebe[89], G. Stoicea[28b], P. Stolte[56],
S. Stonjek[102], A.R. Stradling[8], A. Straessner[46], M.E. Stramaglia[18], J. Strandberg[148],
S. Strandberg[147a,147b], A. Strandlie[120], M. Strauss[114], P. Strizenec[145b], R. Ströhmer[174],
D.M. Strom[117], R. Stroynowski[42], A. Strubig[107], S.A. Stucci[18], B. Stugu[15], N.A. Styles[44],
D. Su[144], J. Su[126], R. Subramaniam[81], S. Suchek[60a], Y. Sugaya[119], M. Suk[129], V.V. Sulin[97],
S. Sultansoy[4c], T. Sumida[70], S. Sun[59], X. Sun[35a], J.E. Sundermann[50], K. Suruliz[150],
G. Susinno[39a,39b], M.R. Sutton[150], S. Suzuki[68], M. Svatos[128], M. Swiatlowski[33], I. Sykora[145a],
T. Sykora[130], D. Ta[50], C. Taccini[135a,135b], K. Tackmann[44], J. Taenzer[159], A. Taffard[163],
R. Tafirout[160a], N. Taiblum[154], H. Takai[27], R. Takashima[71], H. Takeda[69], T. Takeshita[141],
Y. Takubo[68], M. Talby[87], A.A. Talyshev[110,c], J.Y.C. Tam[174], K.G. Tan[90], J. Tanaka[156],
R. Tanaka[118], S. Tanaka[68], B.B. Tannenwald[112], S. Tapia Araya[34b], S. Tapprogge[85], S. Tarem[153],
G.F. Tartarelli[93a], P. Tas[130], M. Tasevsky[128], T. Tashiro[70], E. Tassi[39a,39b],
A. Tavares Delgado[127a,127b], Y. Tayalati[136d], A.C. Taylor[106], G.N. Taylor[90], P.T.E. Taylor[90],
W. Taylor[160b], F.A. Teischinger[32], P. Teixeira-Dias[79], K.K. Temming[50], D. Temple[143],
H. Ten Kate[32], P.K. Teng[152], J.J. Teoh[119], F. Tepel[175], S. Terada[68], K. Terashi[156], J. Terron[84],
S. Terzo[102], M. Testa[49], R.J. Teuscher[159,l], T. Theveneaux-Pelzer[87], J.P. Thomas[19],
J. Thomas-Wilsker[79], E.N. Thompson[37], P.D. Thompson[19], R.J. Thompson[86], A.S. Thompson[55],
L.A. Thomsen[176], E. Thomson[123], M. Thomson[30], M.J. Tibbetts[16], R.E. Ticse Torres[87],
V.O. Tikhomirov[97,am], Yu.A. Tikhonov[110,c], S. Timoshenko[99], P. Tipton[176], S. Tisserant[87],
K. Todome[158], T. Todorov[5,*], S. Todorova-Nova[130], J. Tojo[72], S. Tokár[145a], K. Tokushuku[68],
E. Tolley[59], L. Tomlinson[86], M. Tomoto[104], L. Tompkins[144,an], K. Toms[106], B. Tong[59],
E. Torrence[117], H. Torres[143], E. Torró Pastor[139], J. Toth[87,ao], F. Touchard[87], D.R. Tovey[140],
T. Trefzger[174], A. Tricoli[32], I.M. Trigger[160a], S. Trincaz-Duvoid[82], M.F. Tripiana[13],
W. Trischuk[159], B. Trocmé[57], A. Trofymov[44], C. Troncon[93a], M. Trottier-McDonald[16],
M. Trovatelli[169], L. Truong[164a,164b], M. Trzebinski[41], A. Trzupek[41], J.C-L. Tseng[121],
P.V. Tsiareshka[94], G. Tsipolitis[10], N. Tsirintanis[9], S. Tsiskaridze[13], V. Tsiskaridze[50],
E.G. Tskhadadze[53a], K.M. Tsui[62a], I.I. Tsukerman[98], V. Tsulaia[16], S. Tsuno[68], D. Tsybychev[149],
A. Tudorache[28b], V. Tudorache[28b], A.N. Tuna[59], S.A. Tupputi[22a,22b], S. Turchikhin[100,ak],
D. Turecek[129], D. Turgeman[172], R. Turra[93a,93b], A.J. Turvey[42], P.M. Tuts[37], M. Tyndel[132],
G. Ucchielli[22a,22b], I. Ueda[156], R. Ueno[31], M. Ughetto[147a,147b], F. Ukegawa[161], G. Unal[32],
A. Undrus[27], G. Unel[163], F.C. Ungaro[90], Y. Unno[68], C. Unverdorben[101], J. Urban[145b],
P. Urquijo[90], P. Urrejola[85], G. Usai[8], A. Usanova[64], L. Vacavant[87], V. Vacek[129], B. Vachon[89],
C. Valderanis[101], E. Valdes Santurio[147a,147b], N. Valencic[108], S. Valentinetti[22a,22b], A. Valero[167],
L. Valery[13], S. Valkar[130], S. Vallecorsa[51], J.A. Valls Ferrer[167], W. Van Den Wollenberg[108],
P.C. Van Der Deijl[108], R. van der Geer[108], H. van der Graaf[108], N. van Eldik[153],
P. van Gemmeren[6], J. Van Nieuwkoop[143], I. van Vulpen[108], M.C. van Woerden[32],
M. Vanadia[133a,133b], W. Vandelli[32], R. Vanguri[123], A. Vaniachine[6], P. Vankov[108],
G. Vardanyan[177], R. Vari[133a], E.W. Varnes[7], T. Varol[42], D. Varouchas[82], A. Vartapetian[8],
K.E. Varvell[151], J.G. Vasquez[176], F. Vazeille[36], T. Vazquez Schroeder[89], J. Veatch[56],
L.M. Veloce[159], F. Veloso[127a,127c], S. Veneziano[133a], A. Ventura[75a,75b], M. Venturi[169],
N. Venturi[159], A. Venturini[25], V. Vercesi[122a], M. Verducci[133a,133b], W. Verkerke[108],
J.C. Vermeulen[108], A. Vest[46,ap], M.C. Vetterli[143,d], O. Viazlo[83], I. Vichou[166], T. Vickey[140],
O.E. Vickey Boeriu[140], G.H.A. Viehhauser[121], S. Viel[16], L. Vigani[121], R. Vigne[64], M. Villa[22a,22b],
M. Villaplana Perez[93a,93b], E. Vilucchi[49], M.G. Vincter[31], V.B. Vinogradov[67], C. Vittori[22a,22b],
I. Vivarelli[150], S. Vlachos[10], M. Vlasak[129], M. Vogel[175], P. Vokac[129], G. Volpi[125a,125b], M. Volpi[90],

H. von der Schmitt[102], E. von Toerne[23], V. Vorobel[130], K. Vorobev[99], M. Vos[167], R. Voss[32],
J.H. Vossebeld[76], N. Vranjes[14], M. Vranjes Milosavljevic[14], V. Vrba[128], M. Vreeswijk[108],
R. Vuillermet[32], I. Vukotic[33], Z. Vykydal[129], P. Wagner[23], W. Wagner[175], H. Wahlberg[73],
S. Wahrmund[46], J. Wakabayashi[104], J. Walder[74], R. Walker[101], W. Walkowiak[142],
V. Wallangen[147a,147b], C. Wang[152], C. Wang[35d,87], F. Wang[173], H. Wang[16], H. Wang[42],
J. Wang[44], J. Wang[151], K. Wang[89], R. Wang[6], S.M. Wang[152], T. Wang[23], T. Wang[37],
X. Wang[176], C. Wanotayaroj[117], A. Warburton[89], C.P. Ward[30], D.R. Wardrope[80],
A. Washbrook[48], P.M. Watkins[19], A.T. Watson[19], I.J. Watson[151], M.F. Watson[19], G. Watts[139],
S. Watts[86], B.M. Waugh[80], S. Webb[85], M.S. Weber[18], S.W. Weber[174], J.S. Webster[6],
A.R. Weidberg[121], B. Weinert[63], J. Weingarten[56], C. Weiser[50], H. Weits[108], P.S. Wells[32],
T. Wenaus[27], T. Wengler[32], S. Wenig[32], N. Wermes[23], M. Werner[50], P. Werner[32], M. Wessels[60a],
J. Wetter[162], K. Whalen[117], N.L. Whallon[139], A.M. Wharton[74], A. White[8], M.J. White[1],
R. White[34b], S. White[125a,125b], D. Whiteson[163], F.J. Wickens[132], W. Wiedenmann[173],
M. Wielers[132], P. Wienemann[23], C. Wiglesworth[38], L.A.M. Wiik-Fuchs[23], A. Wildauer[102],
F. Wilk[86], H.G. Wilkens[32], H.H. Williams[123], S. Williams[108], C. Willis[92], S. Willocq[88],
J.A. Wilson[19], I. Wingerter-Seez[5], F. Winklmeier[117], O.J. Winston[150], B.T. Winter[23],
M. Wittgen[144], J. Wittkowski[101], S.J. Wollstadt[85], M.W. Wolter[41], H. Wolters[127a,127c],
B.K. Wosiek[41], J. Wotschack[32], M.J. Woudstra[86], K.W. Wozniak[41], M. Wu[57], M. Wu[33],
S.L. Wu[173], X. Wu[51], Y. Wu[91], T.R. Wyatt[86], B.M. Wynne[48], S. Xella[38], D. Xu[35a], L. Xu[27],
B. Yabsley[151], S. Yacoob[146a], R. Yakabe[69], D. Yamaguchi[158], Y. Yamaguchi[119], A. Yamamoto[68],
S. Yamamoto[156], T. Yamanaka[156], K. Yamauchi[104], Y. Yamazaki[69], Z. Yan[24], H. Yang[35e],
H. Yang[173], Y. Yang[152], Z. Yang[15], W-M. Yao[16], Y.C. Yap[82], Y. Yasu[68], E. Yatsenko[5],
K.H. Yau Wong[23], J. Ye[42], S. Ye[27], I. Yeletskikh[67], A.L. Yen[59], E. Yildirim[44], K. Yorita[171],
R. Yoshida[6], K. Yoshihara[123], C. Young[144], C.J.S. Young[32], S. Youssef[24], D.R. Yu[16], J. Yu[8],
J.M. Yu[91], J. Yu[66], L. Yuan[69], S.P.Y. Yuen[23], I. Yusuff[30,aq], B. Zabinski[41], R. Zaidan[35d],
A.M. Zaitsev[131,ad], N. Zakharchuk[44], J. Zalieckas[15], A. Zaman[149], S. Zambito[59],
L. Zanello[133a,133b], D. Zanzi[90], C. Zeitnitz[175], M. Zeman[129], A. Zemla[40a], J.C. Zeng[166],
Q. Zeng[144], K. Zengel[25], O. Zenin[131], T. Ženiš[145a], D. Zerwas[118], D. Zhang[91], F. Zhang[173],
G. Zhang[35b,al], H. Zhang[35c], J. Zhang[6], L. Zhang[50], R. Zhang[23], R. Zhang[35b,ar], X. Zhang[35d],
Z. Zhang[118], X. Zhao[42], Y. Zhao[35d], Z. Zhao[35b], A. Zhemchugov[67], J. Zhong[121], B. Zhou[91],
C. Zhou[47], L. Zhou[37], L. Zhou[42], M. Zhou[149], N. Zhou[35f], C.G. Zhu[35d], H. Zhu[35a], J. Zhu[91],
Y. Zhu[35b], X. Zhuang[35a], K. Zhukov[97], A. Zibell[174], D. Zieminska[63], N.I. Zimine[67],
C. Zimmermann[85], S. Zimmermann[50], Z. Zinonos[56], M. Zinser[85], M. Ziolkowski[142], L. Živković[14],
G. Zobernig[173], A. Zoccoli[22a,22b], M. zur Nedden[17], G. Zurzolo[105a,105b], L. Zwalinski[32]

1   Department of Physics, University of Adelaide, Adelaide, Australia
2   Physics Department, SUNY Albany, Albany NY, United States of America
3   Department of Physics, University of Alberta, Edmonton AB, Canada
4   (a) Department of Physics, Ankara University, Ankara; (b) Istanbul Aydin University, Istanbul;
    (c) Division of Physics, TOBB University of Economics and Technology, Ankara, Turkey
5   LAPP, CNRS/IN2P3 and Université Savoie Mont Blanc, Annecy-le-Vieux, France
6   High Energy Physics Division, Argonne National Laboratory, Argonne IL, United States of America
7   Department of Physics, University of Arizona, Tucson AZ, United States of America
8   Department of Physics, The University of Texas at Arlington, Arlington TX, United States of
    America
9   Physics Department, University of Athens, Athens, Greece
10 Physics Department, National Technical University of Athens, Zografou, Greece
11 Department of Physics, The University of Texas at Austin, Austin TX, United States of America
12 Institute of Physics, Azerbaijan Academy of Sciences, Baku, Azerbaijan
13 Institut de Física d'Altes Energies (IFAE), The Barcelona Institute of Science and Technology,
    Barcelona, Spain, Spain
14 Institute of Physics, University of Belgrade, Belgrade, Serbia
15 Department for Physics and Technology, University of Bergen, Bergen, Norway

16 Physics Division, Lawrence Berkeley National Laboratory and University of California, Berkeley CA, United States of America

17 Department of Physics, Humboldt University, Berlin, Germany

18 Albert Einstein Center for Fundamental Physics and Laboratory for High Energy Physics, University of Bern, Bern, Switzerland

19 School of Physics and Astronomy, University of Birmingham, Birmingham, United Kingdom

20 [a] Department of Physics, Bogazici University, Istanbul; [b] Department of Physics Engineering, Gaziantep University, Gaziantep; [d] Istanbul Bilgi University, Faculty of Engineering and Natural Sciences, Istanbul,Turkey; [e] Bahcesehir University, Faculty of Engineering and Natural Sciences, Istanbul, Turkey, Turkey

21 Centro de Investigaciones, Universidad Antonio Narino, Bogota, Colombia

22 [a] INFN Sezione di Bologna; [b] Dipartimento di Fisica e Astronomia, Università di Bologna, Bologna, Italy

23 Physikalisches Institut, University of Bonn, Bonn, Germany

24 Department of Physics, Boston University, Boston MA, United States of America

25 Department of Physics, Brandeis University, Waltham MA, United States of America

26 [a] Universidade Federal do Rio De Janeiro COPPE/EE/IF, Rio de Janeiro; [b] Electrical Circuits Department, Federal University of Juiz de Fora (UFJF), Juiz de Fora; [c] Federal University of Sao Joao del Rei (UFSJ), Sao Joao del Rei; [d] Instituto de Fisica, Universidade de Sao Paulo, Sao Paulo, Brazil

27 Physics Department, Brookhaven National Laboratory, Upton NY, United States of America

28 [a] Transilvania University of Brasov, Brasov, Romania; [b] National Institute of Physics and Nuclear Engineering, Bucharest; [c] National Institute for Research and Development of Isotopic and Molecular Technologies, Physics Department, Cluj Napoca; [d] University Politehnica Bucharest, Bucharest; [e] West University in Timisoara, Timisoara, Romania

29 Departamento de Física, Universidad de Buenos Aires, Buenos Aires, Argentina

30 Cavendish Laboratory, University of Cambridge, Cambridge, United Kingdom

31 Department of Physics, Carleton University, Ottawa ON, Canada

32 CERN, Geneva, Switzerland

33 Enrico Fermi Institute, University of Chicago, Chicago IL, United States of America

34 [a] Departamento de Física, Pontificia Universidad Católica de Chile, Santiago; [b] Departamento de Física, Universidad Técnica Federico Santa María, Valparaíso, Chile

35 [a] Institute of High Energy Physics, Chinese Academy of Sciences, Beijing; [b] Department of Modern Physics, University of Science and Technology of China, Anhui; [c] Department of Physics, Nanjing University, Jiangsu; [d] School of Physics, Shandong University, Shandong; [e] Department of Physics and Astronomy, Shanghai Key Laboratory for Particle Physics and Cosmology, Shanghai Jiao Tong University, Shanghai; (also affiliated with PKU-CHEP); [f] Physics Department, Tsinghua University, Beijing 100084, China

36 Laboratoire de Physique Corpusculaire, Clermont Université and Université Blaise Pascal and CNRS/IN2P3, Clermont-Ferrand, France

37 Nevis Laboratory, Columbia University, Irvington NY, United States of America

38 Niels Bohr Institute, University of Copenhagen, Kobenhavn, Denmark

39 [a] INFN Gruppo Collegato di Cosenza, Laboratori Nazionali di Frascati; [b] Dipartimento di Fisica, Università della Calabria, Rende, Italy

40 [a] AGH University of Science and Technology, Faculty of Physics and Applied Computer Science, Krakow; [b] Marian Smoluchowski Institute of Physics, Jagiellonian University, Krakow, Poland

41 Institute of Nuclear Physics Polish Academy of Sciences, Krakow, Poland

42 Physics Department, Southern Methodist University, Dallas TX, United States of America

43 Physics Department, University of Texas at Dallas, Richardson TX, United States of America

44 DESY, Hamburg and Zeuthen, Germany

45 Institut für Experimentelle Physik IV, Technische Universität Dortmund, Dortmund, Germany

46 Institut für Kern- und Teilchenphysik, Technische Universität Dresden, Dresden, Germany

47 Department of Physics, Duke University, Durham NC, United States of America

[48] SUPA — School of Physics and Astronomy, University of Edinburgh, Edinburgh, United Kingdom

[49] INFN Laboratori Nazionali di Frascati, Frascati, Italy

[50] Fakultät für Mathematik und Physik, Albert-Ludwigs-Universität, Freiburg, Germany

[51] Section de Physique, Université de Genève, Geneva, Switzerland

[52] [a] INFN Sezione di Genova; [b] Dipartimento di Fisica, Università di Genova, Genova, Italy

[53] [a] E. Andronikashvili Institute of Physics, Iv. Javakhishvili Tbilisi State University, Tbilisi; [b] High Energy Physics Institute, Tbilisi State University, Tbilisi, Georgia

[54] II Physikalisches Institut, Justus-Liebig-Universität Giessen, Giessen, Germany

[55] SUPA — School of Physics and Astronomy, University of Glasgow, Glasgow, United Kingdom

[56] II Physikalisches Institut, Georg-August-Universität, Göttingen, Germany

[57] Laboratoire de Physique Subatomique et de Cosmologie, Université Grenoble-Alpes, CNRS/IN2P3, Grenoble, France

[58] Department of Physics, Hampton University, Hampton VA, United States of America

[59] Laboratory for Particle Physics and Cosmology, Harvard University, Cambridge MA, United States of America

[60] [a] Kirchhoff-Institut für Physik, Ruprecht-Karls-Universität Heidelberg, Heidelberg; [b] Physikalisches Institut, Ruprecht-Karls-Universität Heidelberg, Heidelberg; [c] ZITI Institut für technische Informatik, Ruprecht-Karls-Universität Heidelberg, Mannheim, Germany

[61] Faculty of Applied Information Science, Hiroshima Institute of Technology, Hiroshima, Japan

[62] [a] Department of Physics, The Chinese University of Hong Kong, Shatin, N.T., Hong Kong; [b] Department of Physics, The University of Hong Kong, Hong Kong; [c] Department of Physics, The Hong Kong University of Science and Technology, Clear Water Bay, Kowloon, Hong Kong, China

[63] Department of Physics, Indiana University, Bloomington IN, United States of America

[64] Institut für Astro- und Teilchenphysik, Leopold-Franzens-Universität, Innsbruck, Austria

[65] University of Iowa, Iowa City IA, United States of America

[66] Department of Physics and Astronomy, Iowa State University, Ames IA, United States of America

[67] Joint Institute for Nuclear Research, JINR Dubna, Dubna, Russia

[68] KEK, High Energy Accelerator Research Organization, Tsukuba, Japan

[69] Graduate School of Science, Kobe University, Kobe, Japan

[70] Faculty of Science, Kyoto University, Kyoto, Japan

[71] Kyoto University of Education, Kyoto, Japan

[72] Department of Physics, Kyushu University, Fukuoka, Japan

[73] Instituto de Física La Plata, Universidad Nacional de La Plata and CONICET, La Plata, Argentina

[74] Physics Department, Lancaster University, Lancaster, United Kingdom

[75] [a] INFN Sezione di Lecce; [b] Dipartimento di Matematica e Fisica, Università del Salento, Lecce, Italy

[76] Oliver Lodge Laboratory, University of Liverpool, Liverpool, United Kingdom

[77] Department of Physics, Jožef Stefan Institute and University of Ljubljana, Ljubljana, Slovenia

[78] School of Physics and Astronomy, Queen Mary University of London, London, United Kingdom

[79] Department of Physics, Royal Holloway University of London, Surrey, United Kingdom

[80] Department of Physics and Astronomy, University College London, London, United Kingdom

[81] Louisiana Tech University, Ruston LA, United States of America

[82] Laboratoire de Physique Nucléaire et de Hautes Energies, UPMC and Université Paris-Diderot and CNRS/IN2P3, Paris, France

[83] Fysiska institutionen, Lunds universitet, Lund, Sweden

[84] Departamento de Fisica Teorica C-15, Universidad Autonoma de Madrid, Madrid, Spain

[85] Institut für Physik, Universität Mainz, Mainz, Germany

[86] School of Physics and Astronomy, University of Manchester, Manchester, United Kingdom

[87] CPPM, Aix-Marseille Université and CNRS/IN2P3, Marseille, France

[88] Department of Physics, University of Massachusetts, Amherst MA, United States of America

[89] Department of Physics, McGill University, Montreal QC, Canada

90 School of Physics, University of Melbourne, Victoria, Australia

91 Department of Physics, The University of Michigan, Ann Arbor MI, United States of America

92 Department of Physics and Astronomy, Michigan State University, East Lansing MI, United States of America

93 (a) INFN Sezione di Milano; (b) Dipartimento di Fisica, Università di Milano, Milano, Italy

94 B.I. Stepanov Institute of Physics, National Academy of Sciences of Belarus, Minsk, Republic of Belarus

95 National Scientific and Educational Centre for Particle and High Energy Physics, Minsk, Republic of Belarus

96 Group of Particle Physics, University of Montreal, Montreal QC, Canada

97 P.N. Lebedev Physical Institute of the Russian Academy of Sciences, Moscow, Russia

98 Institute for Theoretical and Experimental Physics (ITEP), Moscow, Russia

99 National Research Nuclear University MEPhI, Moscow, Russia

100 D.V. Skobeltsyn Institute of Nuclear Physics, M.V. Lomonosov Moscow State University, Moscow, Russia

101 Fakultät für Physik, Ludwig-Maximilians-Universität München, München, Germany

102 Max-Planck-Institut für Physik (Werner-Heisenberg-Institut), München, Germany

103 Nagasaki Institute of Applied Science, Nagasaki, Japan

104 Graduate School of Science and Kobayashi-Maskawa Institute, Nagoya University, Nagoya, Japan

105 (a) INFN Sezione di Napoli; (b) Dipartimento di Fisica, Università di Napoli, Napoli, Italy

106 Department of Physics and Astronomy, University of New Mexico, Albuquerque NM, United States of America

107 Institute for Mathematics, Astrophysics and Particle Physics, Radboud University Nijmegen/Nikhef, Nijmegen, Netherlands

108 Nikhef National Institute for Subatomic Physics and University of Amsterdam, Amsterdam, Netherlands

109 Department of Physics, Northern Illinois University, DeKalb IL, United States of America

110 Budker Institute of Nuclear Physics, SB RAS, Novosibirsk, Russia

111 Department of Physics, New York University, New York NY, United States of America

112 Ohio State University, Columbus OH, United States of America

113 Faculty of Science, Okayama University, Okayama, Japan

114 Homer L. Dodge Department of Physics and Astronomy, University of Oklahoma, Norman OK, United States of America

115 Department of Physics, Oklahoma State University, Stillwater OK, United States of America

116 Palacký University, RCPTM, Olomouc, Czech Republic

117 Center for High Energy Physics, University of Oregon, Eugene OR, United States of America

118 LAL, Univ. Paris-Sud, CNRS/IN2P3, Université Paris-Saclay, Orsay, France

119 Graduate School of Science, Osaka University, Osaka, Japan

120 Department of Physics, University of Oslo, Oslo, Norway

121 Department of Physics, Oxford University, Oxford, United Kingdom

122 (a) INFN Sezione di Pavia; (b) Dipartimento di Fisica, Università di Pavia, Pavia, Italy

123 Department of Physics, University of Pennsylvania, Philadelphia PA, United States of America

124 National Research Centre "Kurchatov Institute" B.P.Konstantinov Petersburg Nuclear Physics Institute, St. Petersburg, Russia

125 (a) INFN Sezione di Pisa; (b) Dipartimento di Fisica E. Fermi, Università di Pisa, Pisa, Italy

126 Department of Physics and Astronomy, University of Pittsburgh, Pittsburgh PA, United States of America

127 (a) Laboratório de Instrumentação e Física Experimental de Partículas — LIP, Lisboa; (b) Faculdade de Ciências, Universidade de Lisboa, Lisboa; (c) Department of Physics, University of Coimbra, Coimbra; (d) Centro de Física Nuclear da Universidade de Lisboa, Lisboa; (e) Departamento de Fisica, Universidade do Minho, Braga; (f) Departamento de Fisica Teorica y del Cosmos and CAFPE, Universidad de Granada, Granada (Spain); (g) Dep Fisica and CEFITEC of Faculdade de Ciencias e Tecnologia, Universidade Nova de Lisboa, Caparica, Portugal

128 Institute of Physics, Academy of Sciences of the Czech Republic, Praha, Czech Republic

129 Czech Technical University in Prague, Praha, Czech Republic

130 Faculty of Mathematics and Physics, Charles University in Prague, Praha, Czech Republic

131 State Research Center Institute for High Energy Physics (Protvino), NRC KI, Russia

132 Particle Physics Department, Rutherford Appleton Laboratory, Didcot, United Kingdom

133 [a] INFN Sezione di Roma; [b] Dipartimento di Fisica, Sapienza Università di Roma, Roma, Italy

134 [a] INFN Sezione di Roma Tor Vergata; [b] Dipartimento di Fisica, Università di Roma Tor Vergata, Roma, Italy

135 [a] INFN Sezione di Roma Tre; [b] Dipartimento di Matematica e Fisica, Università Roma Tre, Roma, Italy

136 [a] Faculté des Sciences Ain Chock, Réseau Universitaire de Physique des Hautes Energies — Université Hassan II, Casablanca; [b] Centre National de l'Energie des Sciences Techniques Nucleaires, Rabat; [c] Faculté des Sciences Semlalia, Université Cadi Ayyad, LPHEA-Marrakech; [d] Faculté des Sciences, Université Mohamed Premier and LPTPM, Oujda; [e] Faculté des sciences, Université Mohammed V, Rabat, Morocco

137 DSM/IRFU (Institut de Recherches sur les Lois Fondamentales de l'Univers), CEA Saclay (Commissariat à l'Energie Atomique et aux Energies Alternatives), Gif-sur-Yvette, France

138 Santa Cruz Institute for Particle Physics, University of California Santa Cruz, Santa Cruz CA, United States of America

139 Department of Physics, University of Washington, Seattle WA, United States of America

140 Department of Physics and Astronomy, University of Sheffield, Sheffield, United Kingdom

141 Department of Physics, Shinshu University, Nagano, Japan

142 Fachbereich Physik, Universität Siegen, Siegen, Germany

143 Department of Physics, Simon Fraser University, Burnaby BC, Canada

144 SLAC National Accelerator Laboratory, Stanford CA, United States of America

145 [a] Faculty of Mathematics, Physics & Informatics, Comenius University, Bratislava; [b] Department of Subnuclear Physics, Institute of Experimental Physics of the Slovak Academy of Sciences, Kosice, Slovak Republic

146 [a] Department of Physics, University of Cape Town, Cape Town; [b] Department of Physics, University of Johannesburg, Johannesburg; [c] School of Physics, University of the Witwatersrand, Johannesburg, South Africa

147 [a] Department of Physics, Stockholm University; [b] The Oskar Klein Centre, Stockholm, Sweden

148 Physics Department, Royal Institute of Technology, Stockholm, Sweden

149 Departments of Physics & Astronomy and Chemistry, Stony Brook University, Stony Brook NY, United States of America

150 Department of Physics and Astronomy, University of Sussex, Brighton, United Kingdom

151 School of Physics, University of Sydney, Sydney, Australia

152 Institute of Physics, Academia Sinica, Taipei, Taiwan

153 Department of Physics, Technion: Israel Institute of Technology, Haifa, Israel

154 Raymond and Beverly Sackler School of Physics and Astronomy, Tel Aviv University, Tel Aviv, Israel

155 Department of Physics, Aristotle University of Thessaloniki, Thessaloniki, Greece

156 International Center for Elementary Particle Physics and Department of Physics, The University of Tokyo, Tokyo, Japan

157 Graduate School of Science and Technology, Tokyo Metropolitan University, Tokyo, Japan

158 Department of Physics, Tokyo Institute of Technology, Tokyo, Japan

159 Department of Physics, University of Toronto, Toronto ON, Canada

160 [a] TRIUMF, Vancouver BC; [b] Department of Physics and Astronomy, York University, Toronto ON, Canada

161 Faculty of Pure and Applied Sciences, and Center for Integrated Research in Fundamental Science and Engineering, University of Tsukuba, Tsukuba, Japan

162 Department of Physics and Astronomy, Tufts University, Medford MA, United States of America

163 Department of Physics and Astronomy, University of California Irvine, Irvine CA, United States of America

164 $^{(a)}$ INFN Gruppo Collegato di Udine, Sezione di Trieste, Udine; $^{(b)}$ ICTP, Trieste; $^{(c)}$ Dipartimento di Chimica, Fisica e Ambiente, Università di Udine, Udine, Italy

165 Department of Physics and Astronomy, University of Uppsala, Uppsala, Sweden

166 Department of Physics, University of Illinois, Urbana IL, United States of America

167 Instituto de Fisica Corpuscular (IFIC) and Departamento de Fisica Atomica, Molecular y Nuclear and Departamento de Ingeniería Electrónica and Instituto de Microelectrónica de Barcelona (IMB-CNM), University of Valencia and CSIC, Valencia, Spain

168 Department of Physics, University of British Columbia, Vancouver BC, Canada

169 Department of Physics and Astronomy, University of Victoria, Victoria BC, Canada

170 Department of Physics, University of Warwick, Coventry, United Kingdom

171 Waseda University, Tokyo, Japan

172 Department of Particle Physics, The Weizmann Institute of Science, Rehovot, Israel

173 Department of Physics, University of Wisconsin, Madison WI, United States of America

174 Fakultät für Physik und Astronomie, Julius-Maximilians-Universität, Würzburg, Germany

175 Fakultät für Mathematik und Naturwissenschaften, Fachgruppe Physik, Bergische Universität Wuppertal, Wuppertal, Germany

176 Department of Physics, Yale University, New Haven CT, United States of America

177 Yerevan Physics Institute, Yerevan, Armenia

178 Centre de Calcul de l'Institut National de Physique Nucléaire et de Physique des Particules (IN2P3), Villeurbanne, France

^{a} Also at Department of Physics, King's College London, London, United Kingdom

^{b} Also at Institute of Physics, Azerbaijan Academy of Sciences, Baku, Azerbaijan

^{c} Also at Novosibirsk State University, Novosibirsk, Russia

^{d} Also at TRIUMF, Vancouver BC, Canada

^{e} Also at Department of Physics & Astronomy, University of Louisville, Louisville, KY, United States of America

^{f} Also at Department of Physics, California State University, Fresno CA, United States of America

^{g} Also at Department of Physics, University of Fribourg, Fribourg, Switzerland

^{h} Also at Departament de Fisica de la Universitat Autonoma de Barcelona, Barcelona, Spain

^{i} Also at Departamento de Fisica e Astronomia, Faculdade de Ciencias, Universidade do Porto, Portugal

^{j} Also at Tomsk State University, Tomsk, Russia

^{k} Also at Universita di Napoli Parthenope, Napoli, Italy

^{l} Also at Institute of Particle Physics (IPP), Canada

^{m} Also at Department of Physics, St. Petersburg State Polytechnical University, St. Petersburg, Russia

^{n} Also at Department of Physics, The University of Michigan, Ann Arbor MI, United States of America

^{o} Also at Centre for High Performance Computing, CSIR Campus, Rosebank, Cape Town, South Africa

^{p} Also at Louisiana Tech University, Ruston LA, United States of America

^{q} Also at Institucio Catalana de Recerca i Estudis Avancats, ICREA, Barcelona, Spain

^{r} Also at Graduate School of Science, Osaka University, Osaka, Japan

^{s} Also at Department of Physics, National Tsing Hua University, Taiwan

^{t} Also at Institute for Mathematics, Astrophysics and Particle Physics, Radboud University Nijmegen/Nikhef, Nijmegen, Netherlands

^{u} Also at Department of Physics, The University of Texas at Austin, Austin TX, United States of America

^{v} Also at Institute of Theoretical Physics, Ilia State University, Tbilisi, Georgia

^{w} Also at CERN, Geneva, Switzerland

^{x} Also at Georgian Technical University (GTU),Tbilisi, Georgia

^{y} Also at Ochadai Academic Production, Ochanomizu University, Tokyo, Japan

^{z} Also at Manhattan College, New York NY, United States of America

^{aa} Also at Hellenic Open University, Patras, Greece

^{ab} Also at Academia Sinica Grid Computing, Institute of Physics, Academia Sinica, Taipei, Taiwan

^{ac} Also at School of Physics, Shandong University, Shandong, China

^{ad} Also at Moscow Institute of Physics and Technology State University, Dolgoprudny, Russia

^{ae} Also at section de Physique, Université de Genève, Geneva, Switzerland

^{af} Also at Eotvos Lorand University, Budapest, Hungary

^{ag} Also at International School for Advanced Studies (SISSA), Trieste, Italy

^{ah} Also at Department of Physics and Astronomy, University of South Carolina, Columbia SC, United States of America

^{ai} Also at School of Physics and Engineering, Sun Yat-sen University, Guangzhou, China

^{aj} Also at Institute for Nuclear Research and Nuclear Energy (INRNE) of the Bulgarian Academy of Sciences, Sofia, Bulgaria

^{ak} Also at Faculty of Physics, M.V.Lomonosov Moscow State University, Moscow, Russia

^{al} Also at Institute of Physics, Academia Sinica, Taipei, Taiwan

^{am} Also at National Research Nuclear University MEPhI, Moscow, Russia

^{an} Also at Department of Physics, Stanford University, Stanford CA, United States of America

^{ao} Also at Institute for Particle and Nuclear Physics, Wigner Research Centre for Physics, Budapest, Hungary

^{ap} Also at Flensburg University of Applied Sciences, Flensburg, Germany

^{aq} Also at University of Malaya, Department of Physics, Kuala Lumpur, Malaysia

^{ar} Also at CPPM, Aix-Marseille Université and CNRS/IN2P3, Marseille, France

* Deceased